Study of freeze-out, directed flow and vorticity in heavy-ion collisions at NICA energies

L. Bravina,

in collaboration with

O. Vitiuk and E. Zabrodin

ICNFP-2021, OAC, Kolymbari, Crete, Greece, 23.08. – 02.09.2021

Outline

I. Motivation

II. Chemical and thermal freeze-out of main hadron species

III. Spatial separation of different species. Consequences for

- Thermal Model predictions of yields
- directed flow of different particles
- thermal vorticity
- Lambda and anti-Lambda polarization
- femtoscopy correlations

IV. Conclusions

I. Motivation

Dynamic Regimes

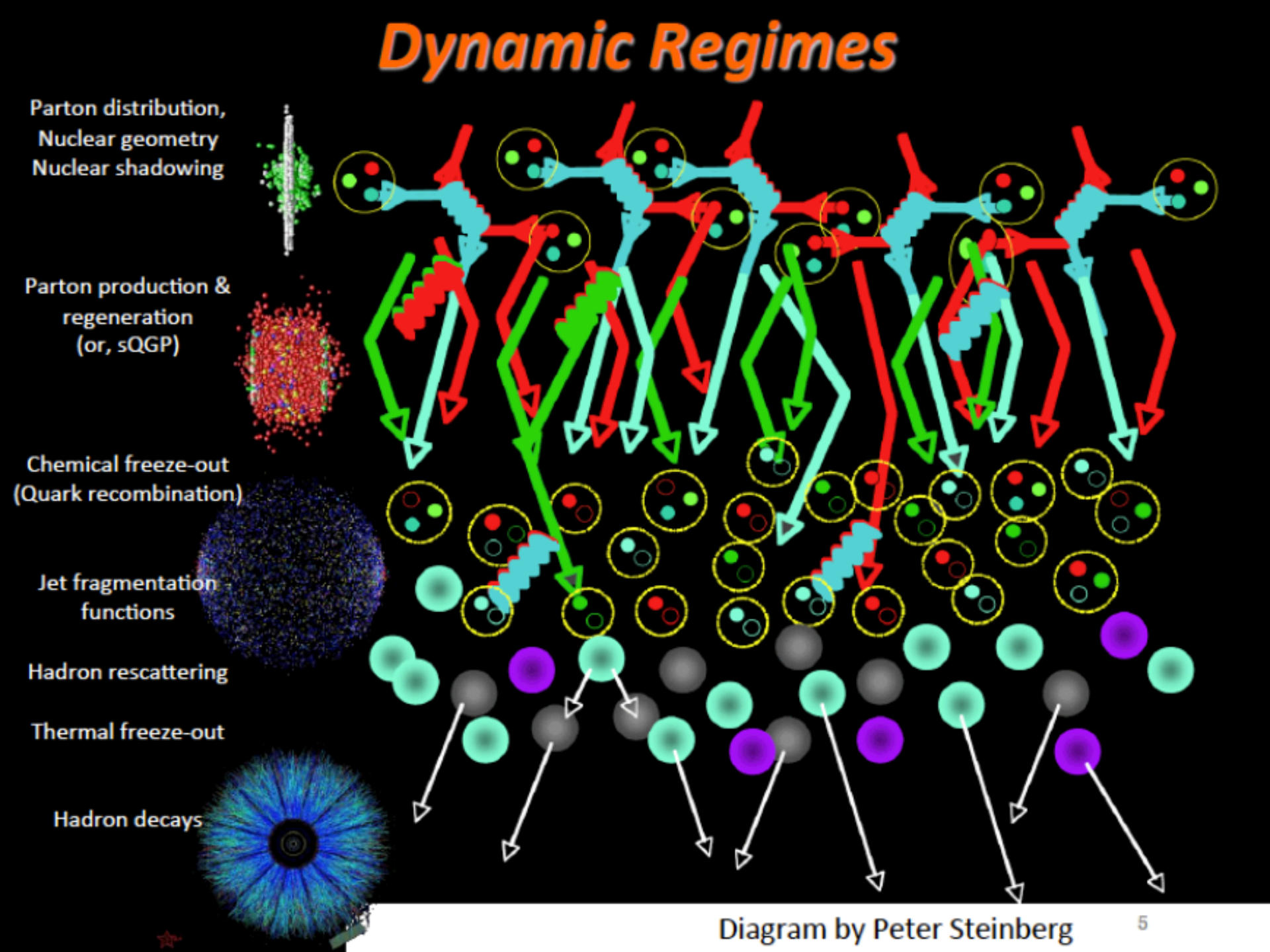

Diagram by Peter Steinberg

Motivation

1. Flavor dependent Freeze-out temperatu

In the crossover region of QCD phase diagr

F.A. Flor, G. Olinger, R. Bellwied ArXiv: 20

T_u,d = 150 MeV, T_s= 165 MeV

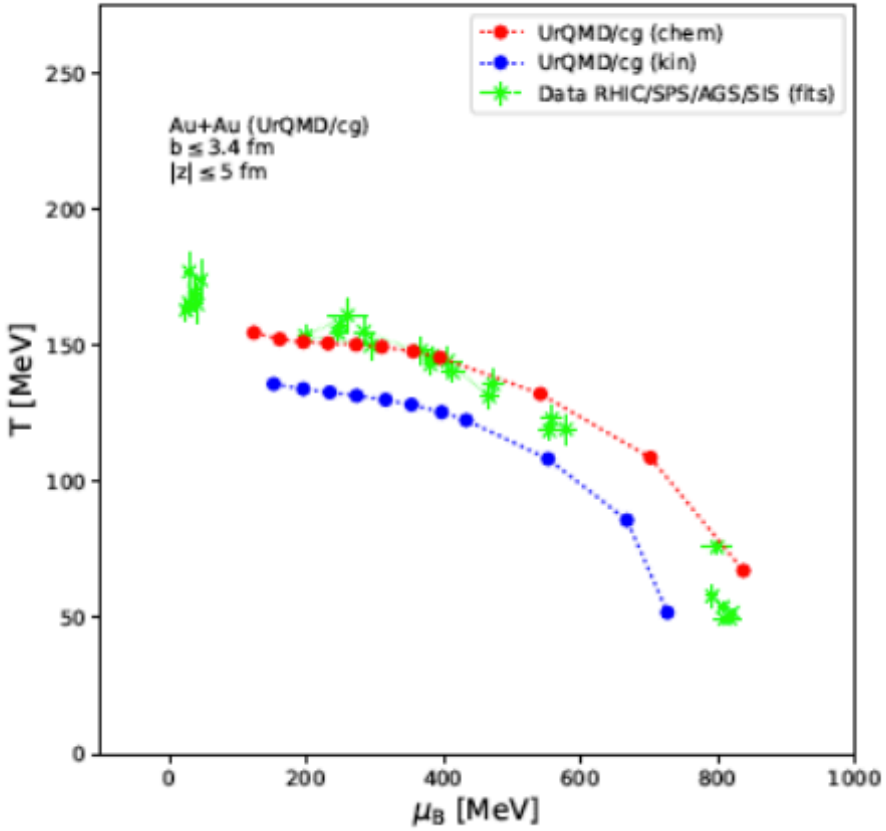

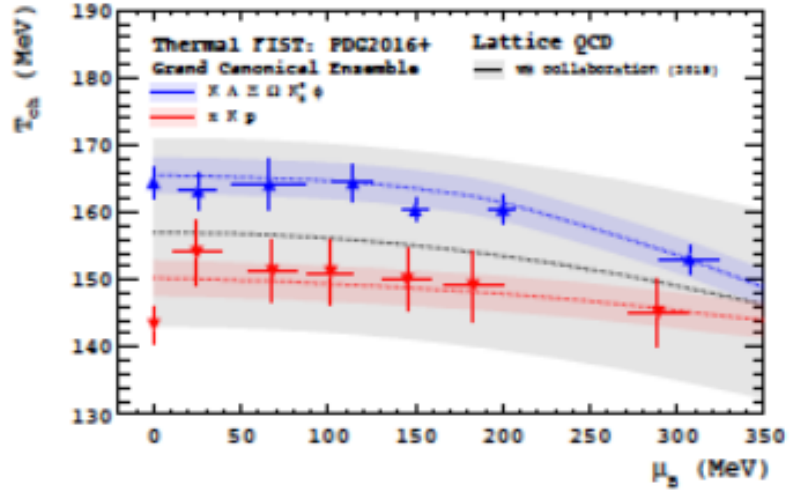

FIG. 2: *Strange* (blue points) and *light* (red points) GCE fits to STAR and ALICE data measured at collision energies ranging from $\sqrt{s_{NN}} = 11.5$ GeV to 5.02 TeV (0 - 10%) via The FIST using the PDG2016+ hadronic spectrum.

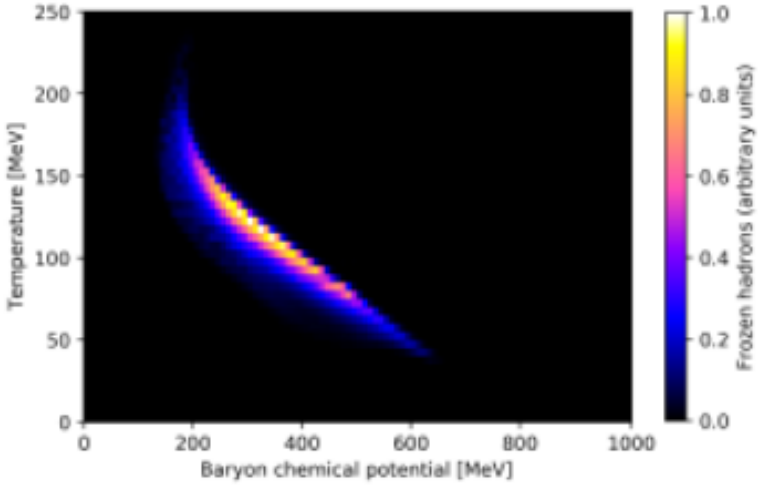

Figure 12. (Color online) Profile of the kinetic freeze-out temperature and baryon chemical potential at $|y| < 0.2$ for Au+Au collisions at $\sqrt{s_{NN}} = 19.6$ GeV.

Motivation

Au+Au at $E_{lab} = 40$A GeV and $b = 0$ fm within UrQMD

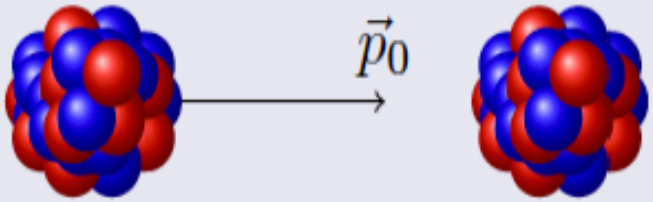

- To do the analysis of the spatio-temporal evolution of all particles in the $T - \mu_B$, $T - \mu_S$ plane and the analysis of the finally emitted particles in $x - t$ plane.
- See the spatial separation of strange particles from non strange (and of mesons from baryons).
- Find average T, μ_B, μ_S of different particles at freeze-out time.

Identified hadron yields

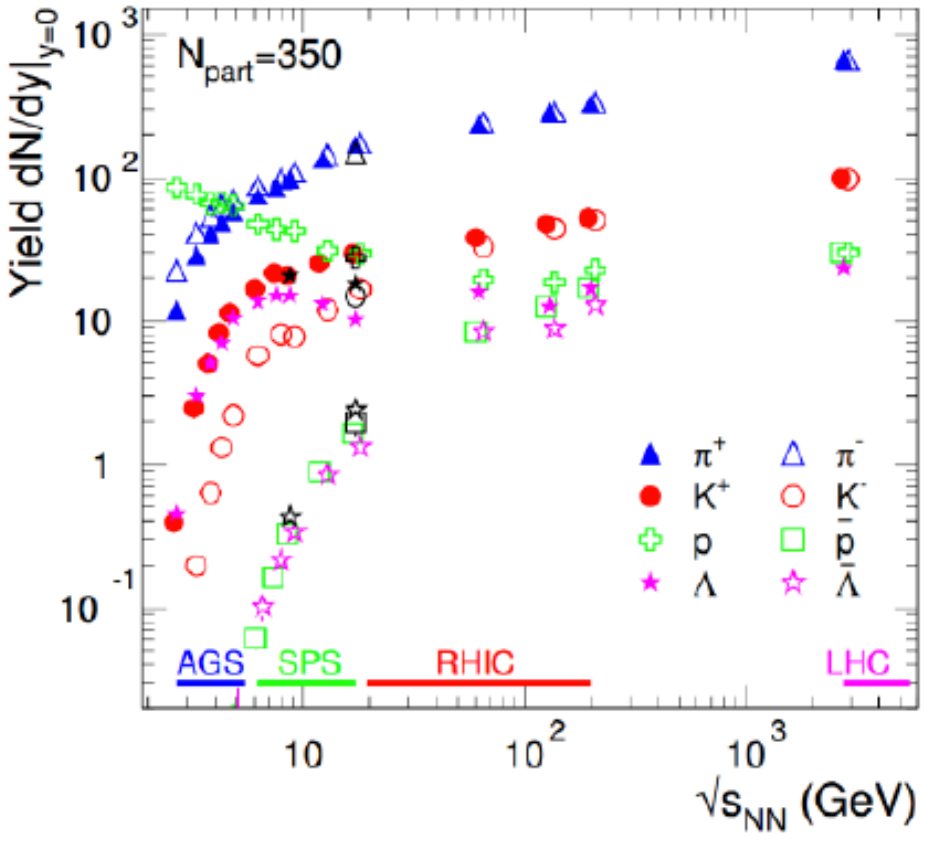

- Lots of particles, most newly created from the excited gluon fields ($E=mc^2$)
- Large variety of species:

  $\pi^{\pm}(u\bar{d},d\bar{u})$, m=140 MeV

  $K^{\pm}(u\bar{s},s\bar{u})$, m=494 MeV

  p(uud), m=938 MeV

  Λ(uds), m=1116 MeV

  also: Ξ(dss), Ω(sss), …
- Abundancies follow mass hierarchy, except at low energies where remnants from the incoming nuclei are significant
- What do we learn?

Grand Canonical Ensemble

$$\ln Z_i = \frac{V g_i}{2\pi^2} \int_0^\infty \pm p^2 dp \ln(1 \pm \exp(-(E_i - \mu_i)/T))$$

$$n_i = N/V = -\frac{T}{V}\frac{\partial \ln Z_i}{\partial \mu} = \frac{g_i}{2\pi^2} \int_0^\infty \frac{p^2\,\mathrm{d}p}{\exp((E_i - \mu_i)/T) \pm 1}$$

$$\mu_i = \mu_B B_i + \mu_S S_i + \mu_{I_3} I_i^3$$

Fit at each energy provides values for T and μ_b

for every conserved quantum number there is a chemical potential μ
but can use conservation laws to constrain:

- Baryon number: $V \sum_i n_i B_i = Z + N \quad \rightarrow V$
- Strangeness: $V \sum_i n_i S_i - 0 \quad \rightarrow \mu_S$
- Charge: $V \sum_i n_i I_i^3 = \frac{Z - N}{2} \quad \rightarrow \mu_{I_3}$

This leaves only μ_b and T as free parameter when 4π considered
for rapidity slice fix volume e.g. by dN_{ch}/dy

Chemical freeze-out

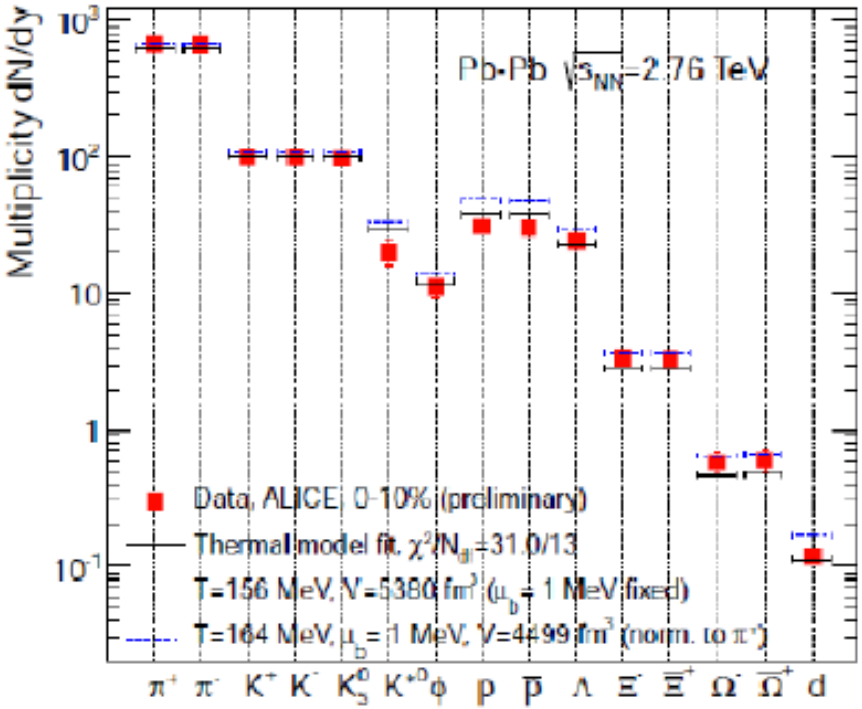

- Thermal fits of hadron abundancies:

$$n_i = N_i/V = -\frac{T}{V}\frac{\partial \ln Z_i}{\partial \mu} = \frac{g_i}{2\pi^2}\int_0^\infty \frac{p^2 \mathrm{d}p}{\exp[(E_i-\mu_i)/T] \pm 1}$$

- Quantum numbers conservation

  $\mu=\mu_B B+\mu_{I3} I_3+\mu_S S+\mu_C C$

- Hadron yields N_i can be obtained using only 3 parameters: (T_{chem},μ_B, V)

- The hadron abundancies are in agreement with a thermally equilibrated system

  T_{chem}=155-165 MeV

  μ_B~0

Central cell: Relaxation to (local) equilibrium

Equilibration in the Central Cell

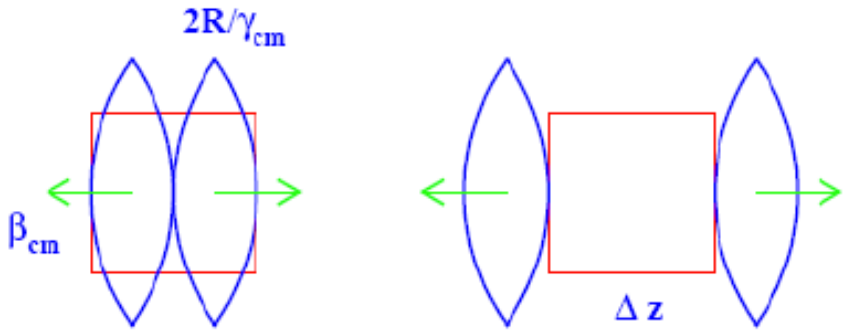

$t^{cross} = 2R/(\gamma_{cm}\,\beta_{cm})$ $\qquad$ $t^{eq} \geq t^{cross} + \Delta z/(2\beta_{cm})$

Kinetic equilibrium:

Isotropy of velocity distributions

Isotropy of pressure

Thermal equilibrium:

Energy spectra of particles are described by Boltzmann distribution

L.Bravina et al., PLB 434 (1998) 379; JPG 25 (1999) 351

$$\frac{dN_i}{4\pi p E dE} = \frac{V g_i}{(2\pi\hbar)^3} \exp\left(\frac{\mu_i}{T}\right) \exp\left(-\frac{E_i}{T}\right)$$

Chemical equlibrium:

Particle yields are reproduced by SM with the same values of $(T,\ \mu_B,\ \mu_S)$:

$$N_i = \frac{V g_i}{2\pi^2\hbar^3} \int_0^\infty p^2 dp \exp\left(\frac{\mu_i}{T}\right) \exp\left(-\frac{E_i}{T}\right)$$

Statistical model of ideal hadron gas

input values

output values

$$\varepsilon^{\rm mic} = \frac{1}{V}\sum_i E_i^{\rm SM}(T,\mu_{\rm B},\mu_{\rm S}),$$

$$\rho_{\rm B}^{\rm mic} = \frac{1}{V}\sum_i B_i\cdot N_i^{\rm SM}(T,\mu_{\rm B},\mu_{\rm S}),$$

$$\rho_{\rm S}^{\rm mic} = \frac{1}{V}\sum_i S_i\cdot N_i^{\rm SM}(T,\mu_{\rm B},\mu_{\rm S}).$$

Multiplicity

Energy

Pressure

Entropy density

$$N_i^{\rm SM} = \frac{Vg_i}{2\pi^2\hbar^3}\int_0^\infty p^2 f(p,m_i)dp,$$

$$E_i^{\rm SM} = \frac{Vg_i}{2\pi^2\hbar^3}\int_0^\infty p^2\sqrt{p^2+m_i^2}\, f(p,m_i)dp$$

$$P^{\rm SM} = \sum_i \frac{g_i}{2\pi^2\hbar^3}\int_0^\infty p^2\frac{p^2}{3(p^2+m_i^2)^{1/2}}\, f(p,m_i)dp$$

$$s^{\rm SM} = -\sum_i \frac{g_i}{2\pi^2\hbar^3}\int_0^\infty f(p,m_i)\,[\ln f(p,m_i)-1]\,p^2dp$$

Kinetic Equilibrium

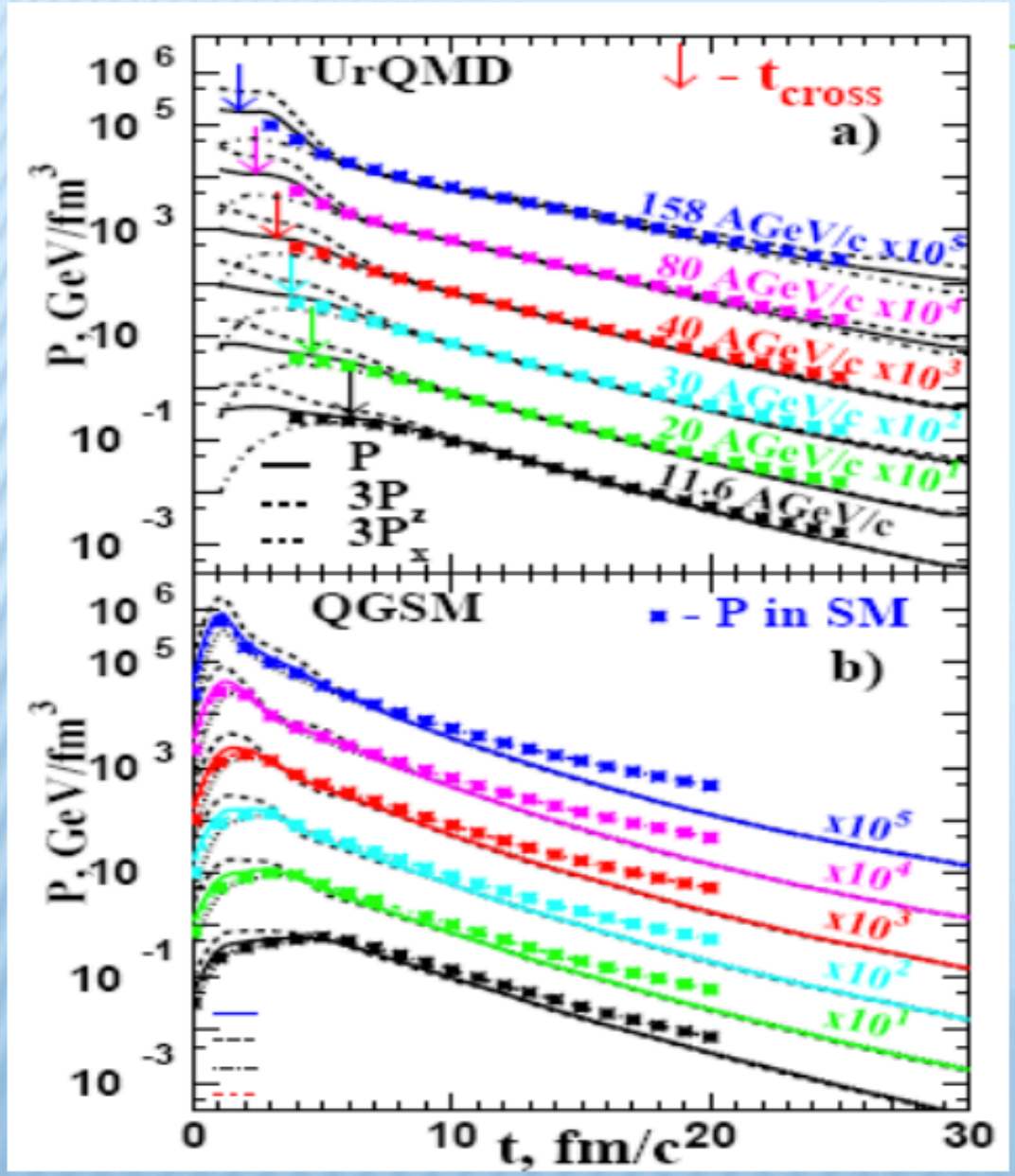

Isotropy of pressure

L.Bravina et al.,
PRC 78 (2008) 014907

Pressure becomes isotropic for all energies from 11.6 AGeV to 158 AGeV

NEGATIVE NET STRANGENESS DENSITY

Net strangeness density in the central cell at 11 to 80 AGeV

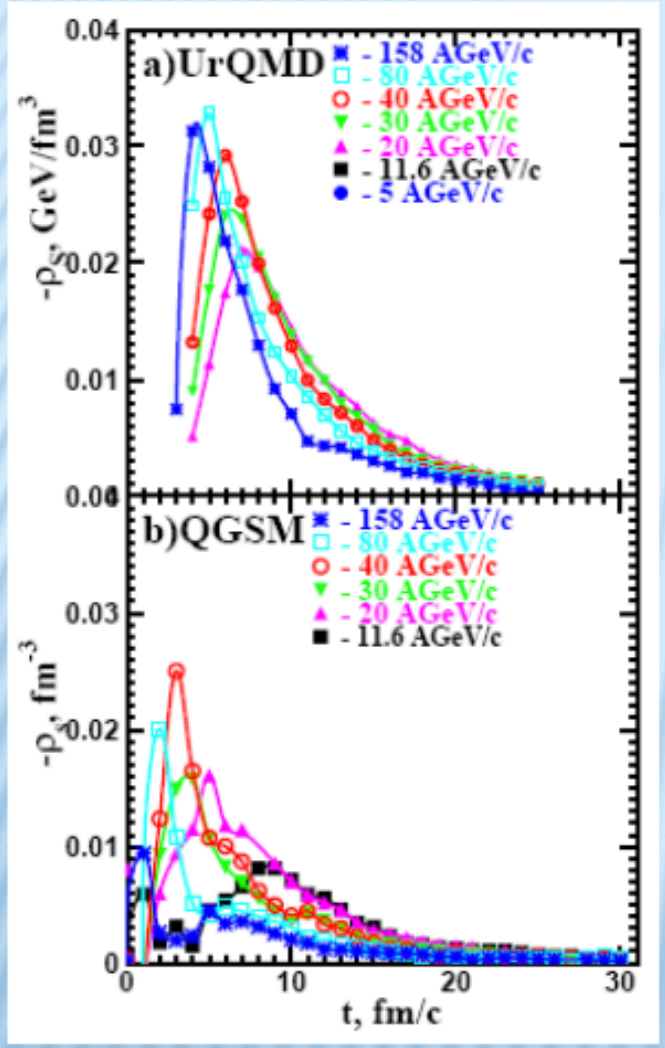

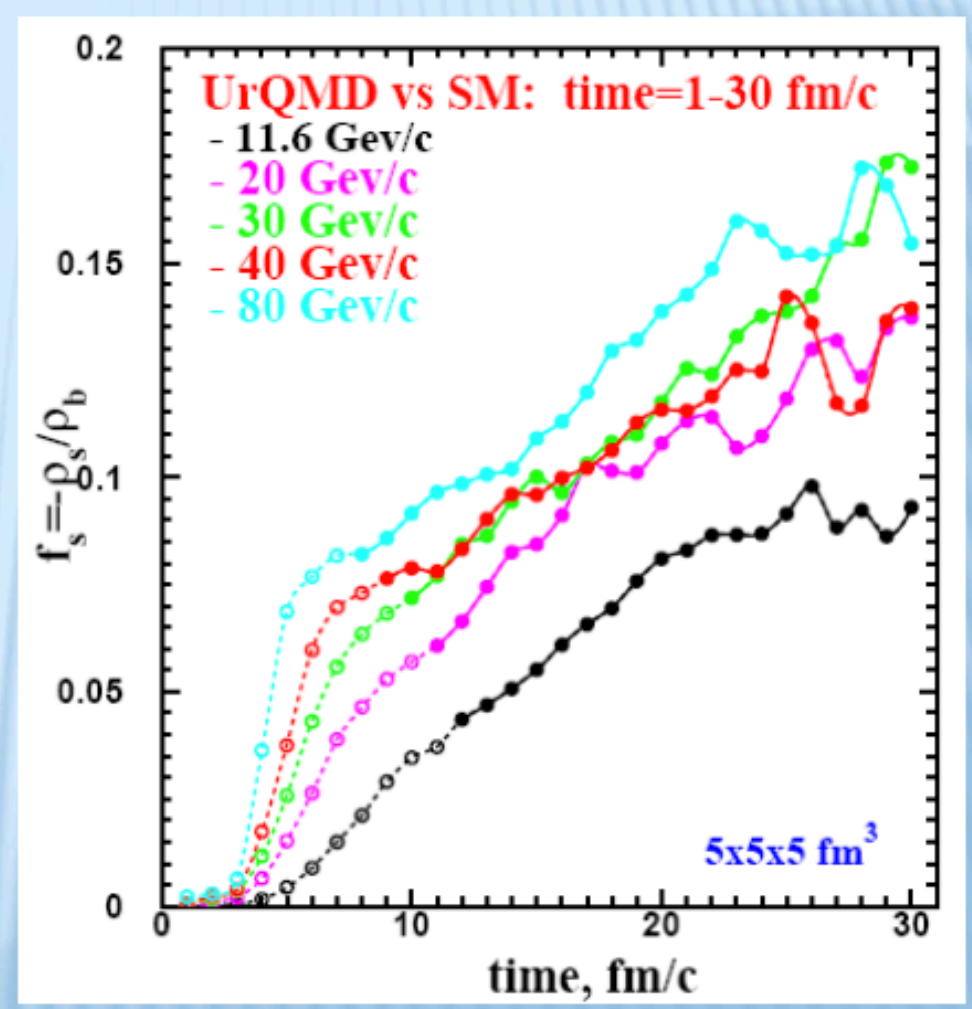

Net strangeness in the cell is negative because of different interaction cross sections for Kaons and antiKaons with Baryons

THERMAL AND CHEMICAL EQUILIBRIUM

Boltzmann fit to the energy spectra

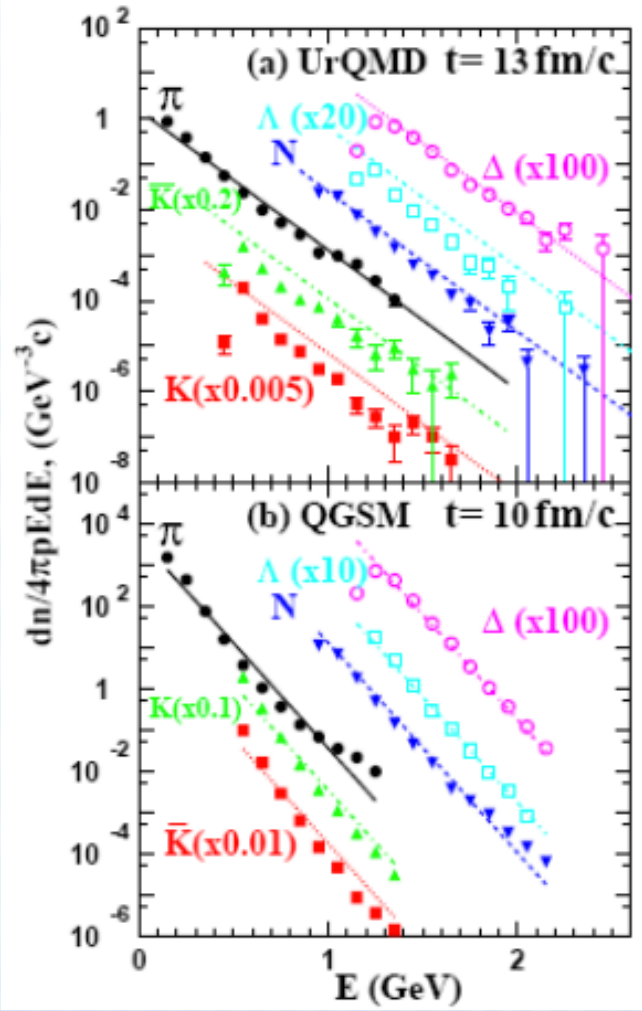

PRC 78 (2008) 014907

Particle yields

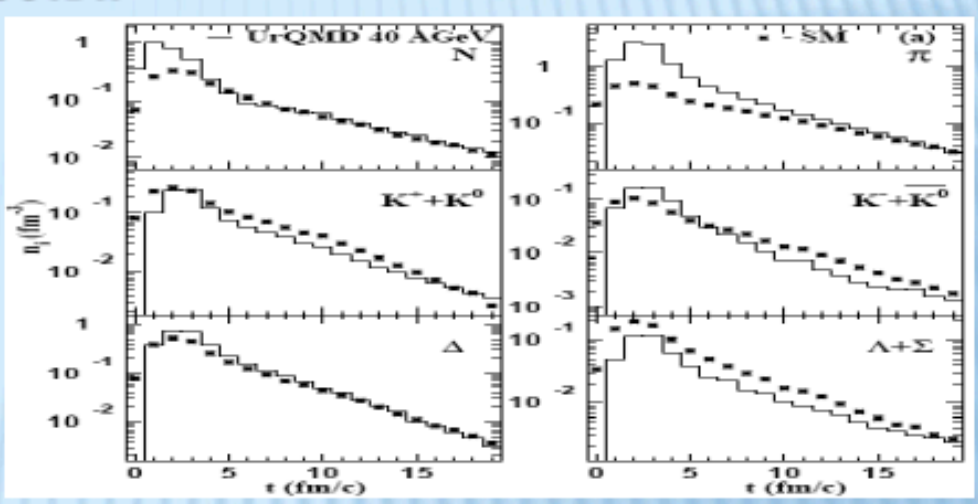

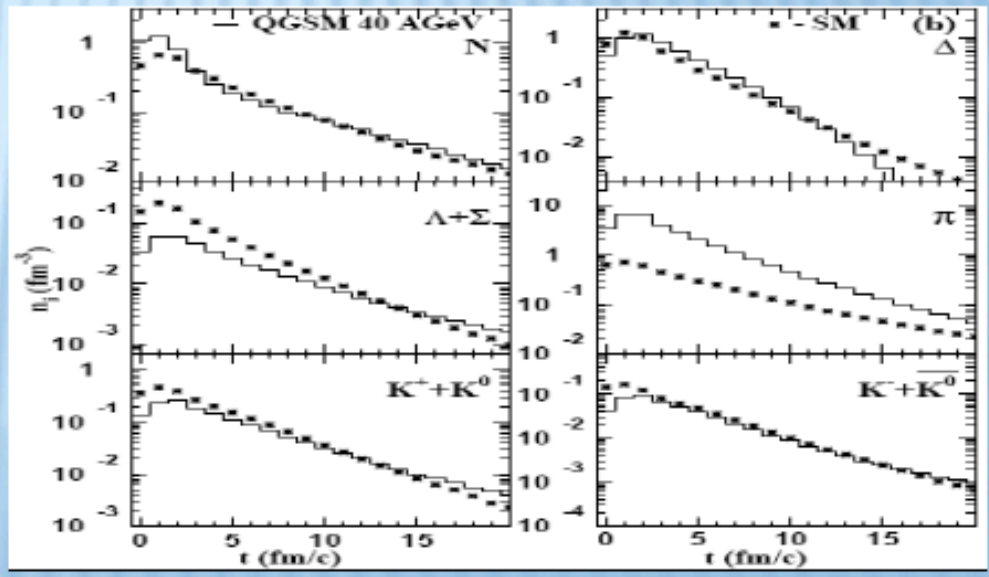

Thermal and chemical equilibrium seems to be reached

HOW DENSE CAN BE THE MEDIUM?

PRC 78 (2008) 014907

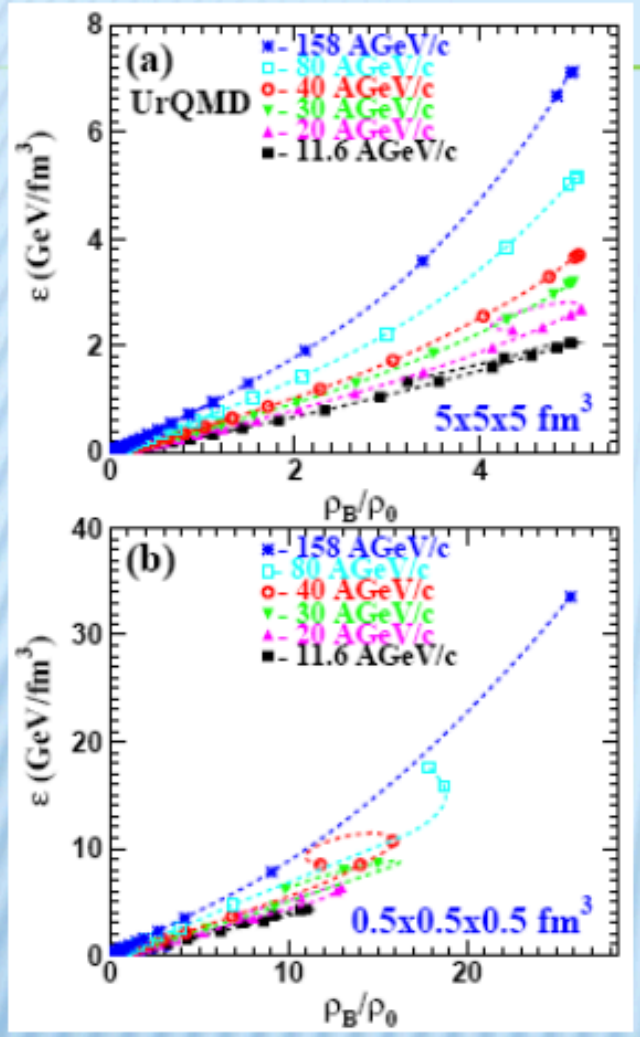

"Big" cell (V = 5x5x5 fm^3)

"Small" cell (V => 0)

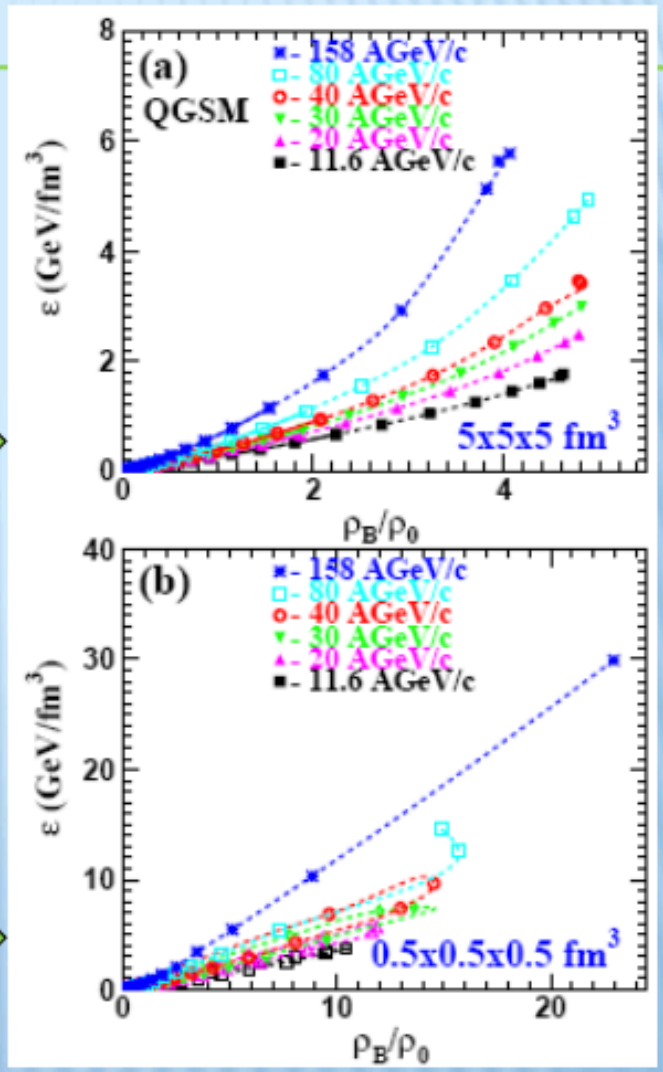

Dramatic differences at the non-equilibrium stage; after beginning of kinetic equilibrium the energy densities and the baryon densities are the same for "small" and "big" cell

COMPARISON BETWEEN MODELS

The phase trajectories at the center of a head-on Au+Au collisions

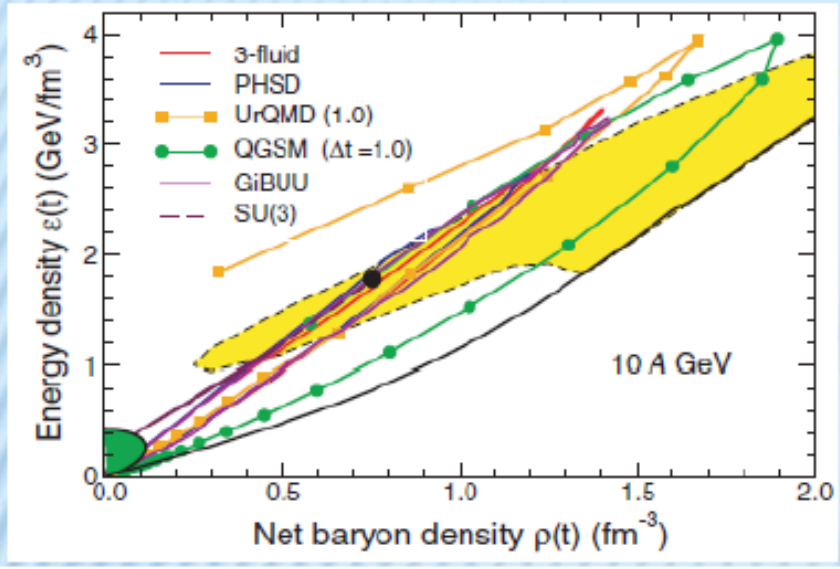

I. Arsene et al., PRC 75 (2007) 034902

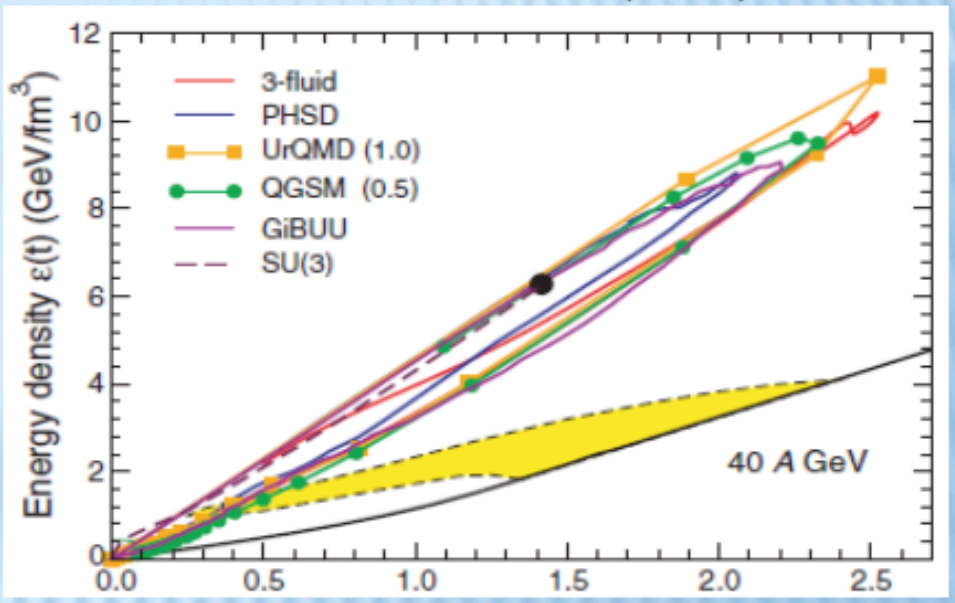

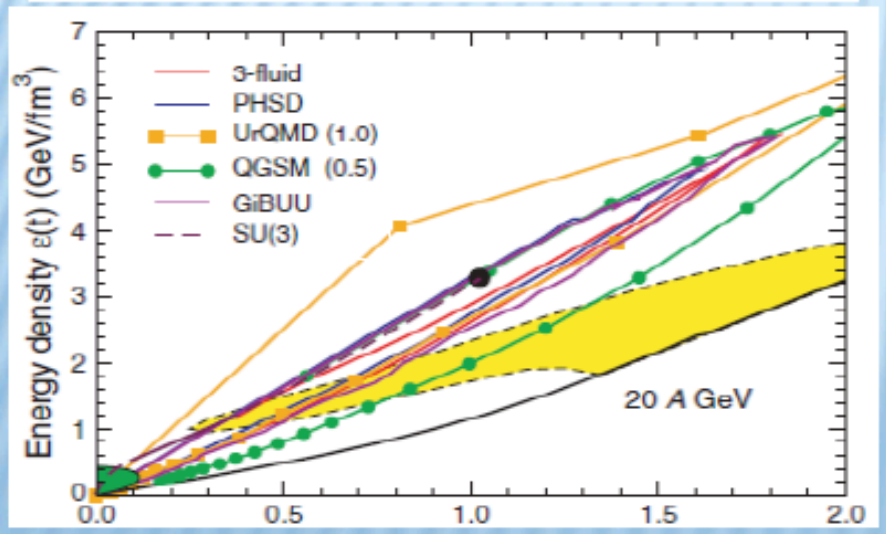

Green area : freeze-out region;
Yellow area : the phase coexistence region from schematic EOS that has a critical point at final density

Different models exhibit a large degree of mutual agreement

II. Chemical and Thermal Freeze-out of Main Hadron Species

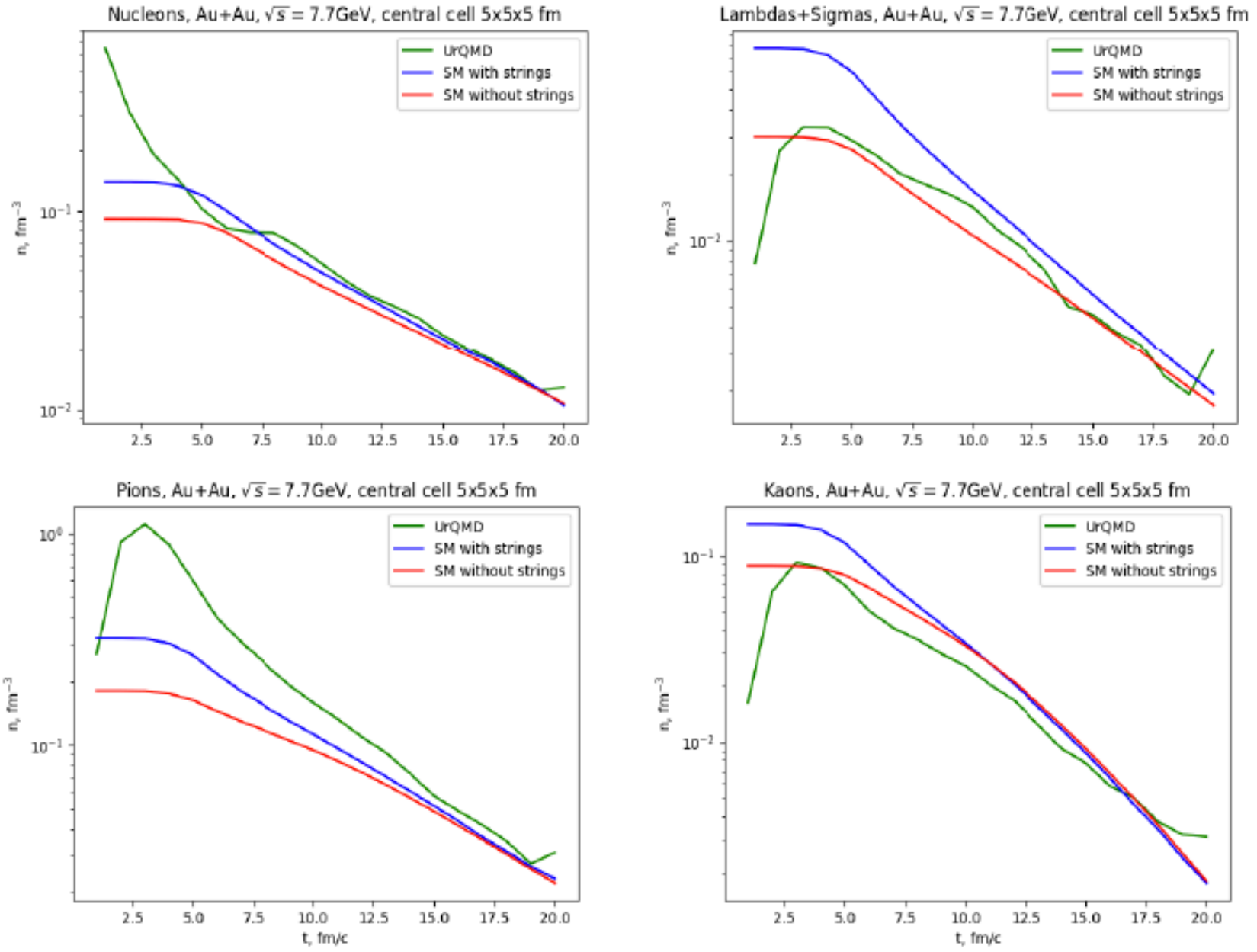

Figure 1: Particle densities in the central cell at times 1 – 20 fm/c.

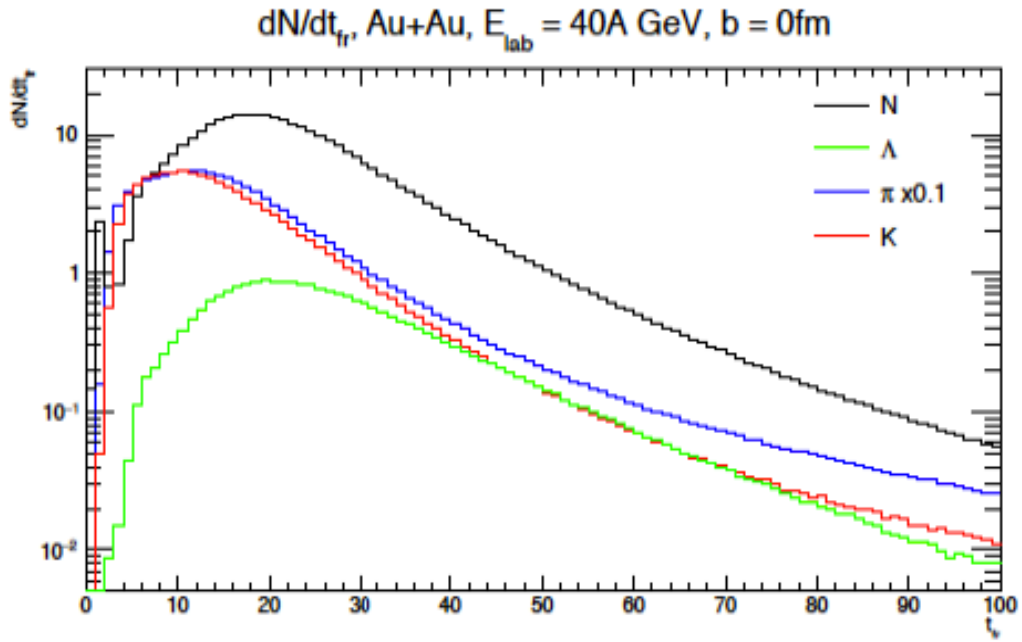

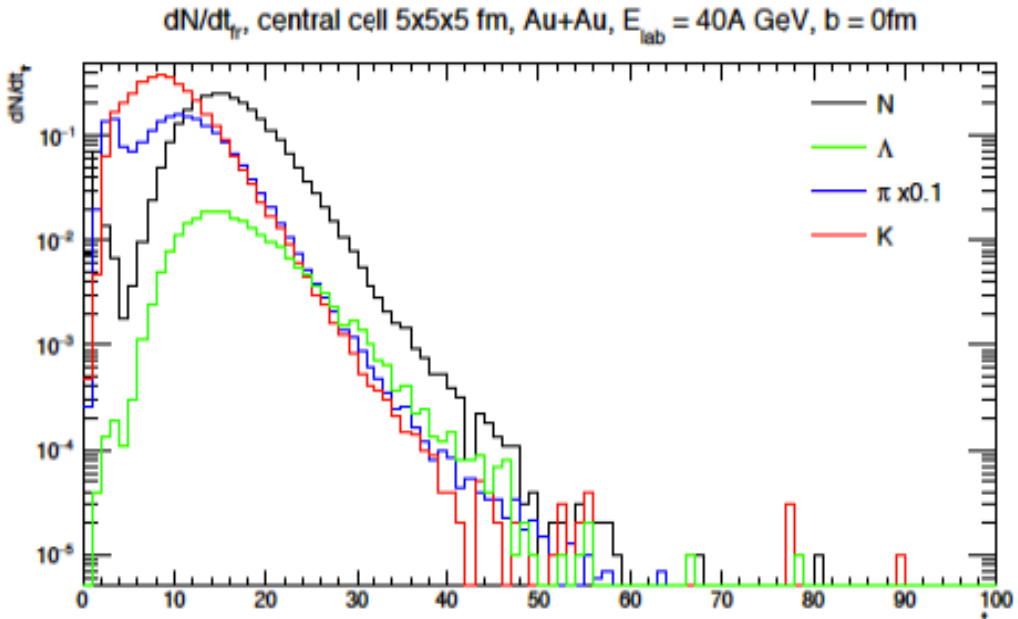

Different particles are frozen at different space - times with different values of T-μ_B-μ_S

Figure 3: dN/dt_{fr} for all space and for central cell.

Au+Au, E_{lab}=10A GeV, b = 0 fm, all space

	All y						$\|y\| < 1$					
	t, fm/c	$\|x\|, \|y\|$, fm	$\|z\|$, fm	T, MeV	μ_b, MeV	μ_s, MeV	t, fm/c	$\|x\|, \|y\|$, fm	$\|z\|$, fm	T, MeV	μ_b, MeV	μ_s, MeV
All	18.0	4.7	6.4	112.4	473.1	72.1	18.1	4.9	5.3	110.6	492.3	70.8
p	19.7	4.7	7.2	108.6	478.1	63.0	19.6	4.9	5.7	101.9	524.5	72.5
$\overline{p}$	19.1	5.9	7.8	109.0	459.1	64.5	18.3	6.4	5.8	106.1	462.1	66.6
Λ	24.6	5.5	8.1	90.4	539.8	50.4	24.4	5.7	7.1	92.2	532.3	49.4
$\overline{\Lambda}$	23.3	6.6	8.6	98.2	487.0	58.0	22.7	6.8	7.2	96.4	497.4	54.1
Σ	20.4	4.7	6.4	105.0	496.4	56.8	20.3	4.8	5.7	101.9	524.5	72.5
$\overline{\Sigma}$	20.0	5.5	7.5	106.3	472.7	62.3	19.5	5.7	6.4	104.0	489.4	62.4
π	16.9	4.7	6.1	116.8	448.5	69.0	17.0	4.9	5.1	114.6	471.2	73.4
K	14.4	3.7	4.4	128.1	457.4	83.5	14.4	3.9	3.8	124.8	486.1	93.8
$\overline{K}$	20.9	5.3	7.1	102.9	486.2	59.9	20.8	5.5	6.1	101.0	500.6	64.8

Table 1: Average coordinates of freezeout and T, μ_b, μ_s at this coordinates.

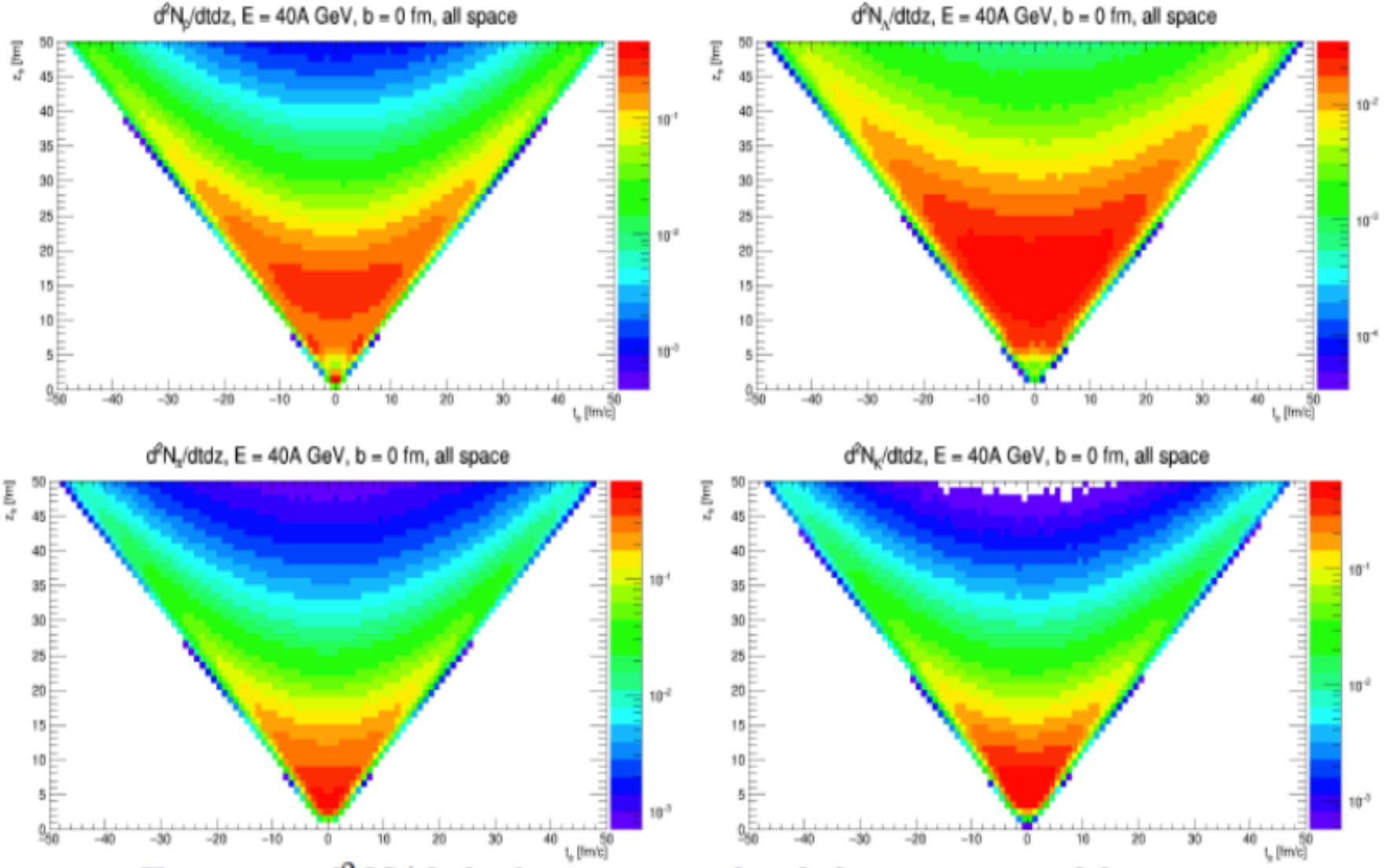

Figure 4: $d^2N/dtdz$ for protons, lambdas, pions and kaons.

Freeze-out

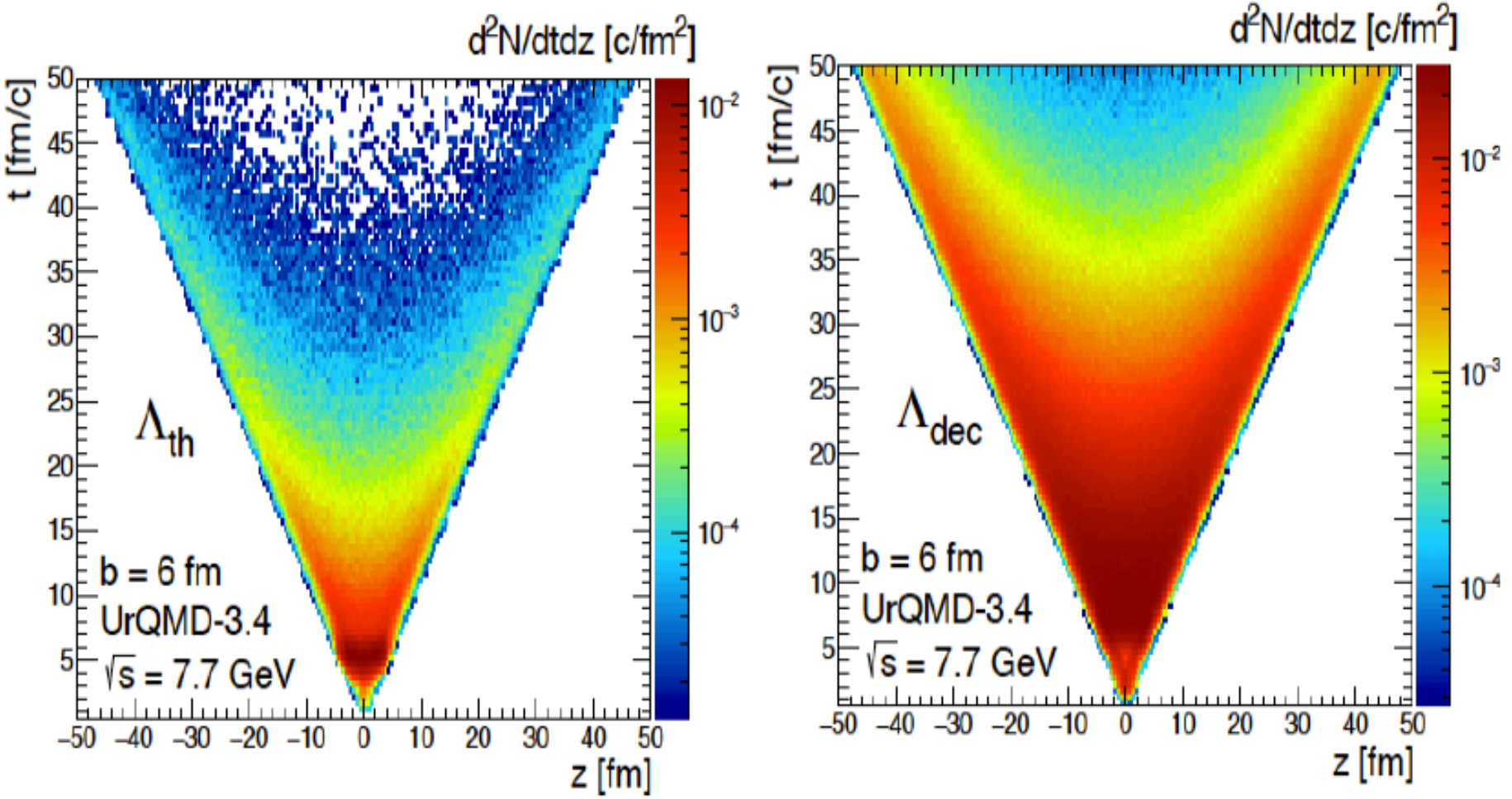

$d^2N/dtdz$ distribution of the final state hadrons over their formation point in (t, z) plane at $\sqrt{s} = 7.7\ GeV$ (left), $\sqrt{s} = 19.6\ GeV$ (right), $b = 6\ fm$.

Freeze-out

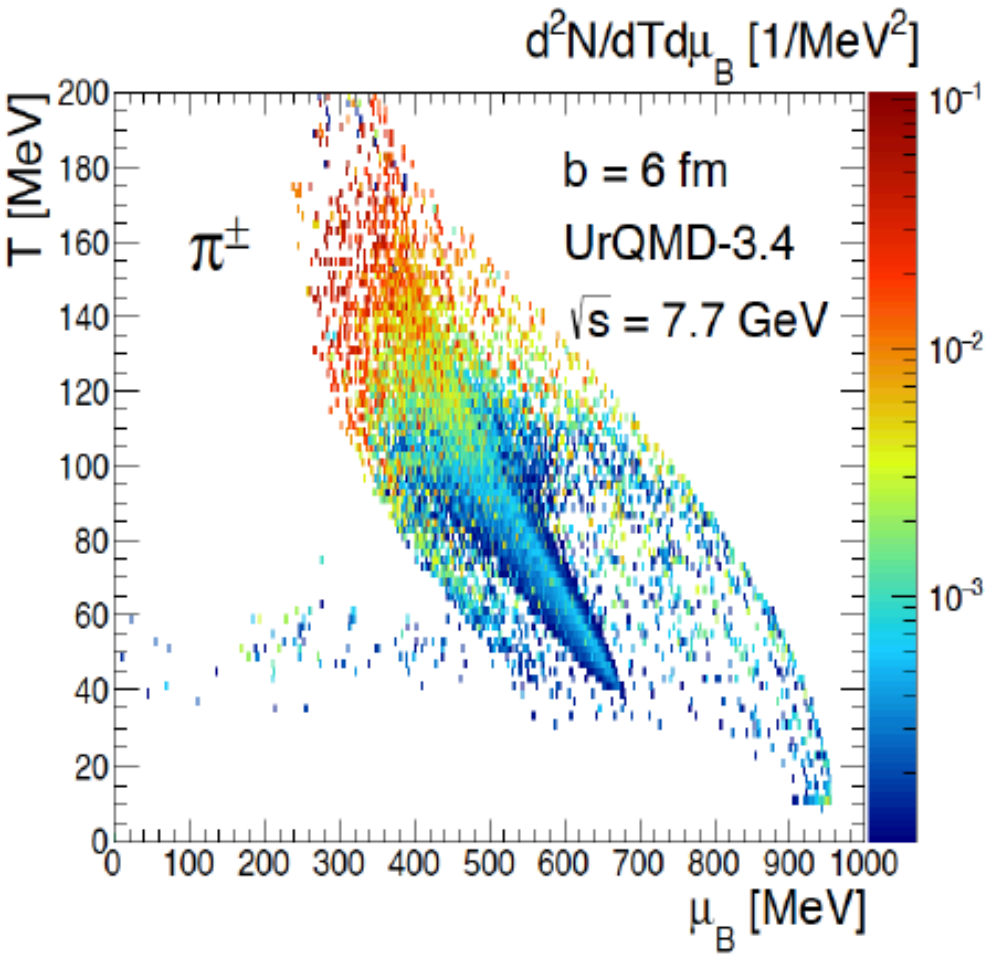

$d^2N/dTd\mu_B$ distribution of the final state hadr

(T, mu_B) plane at $\sqrt{s} = 7.7\ GeV,\ b = 6\ fm.$

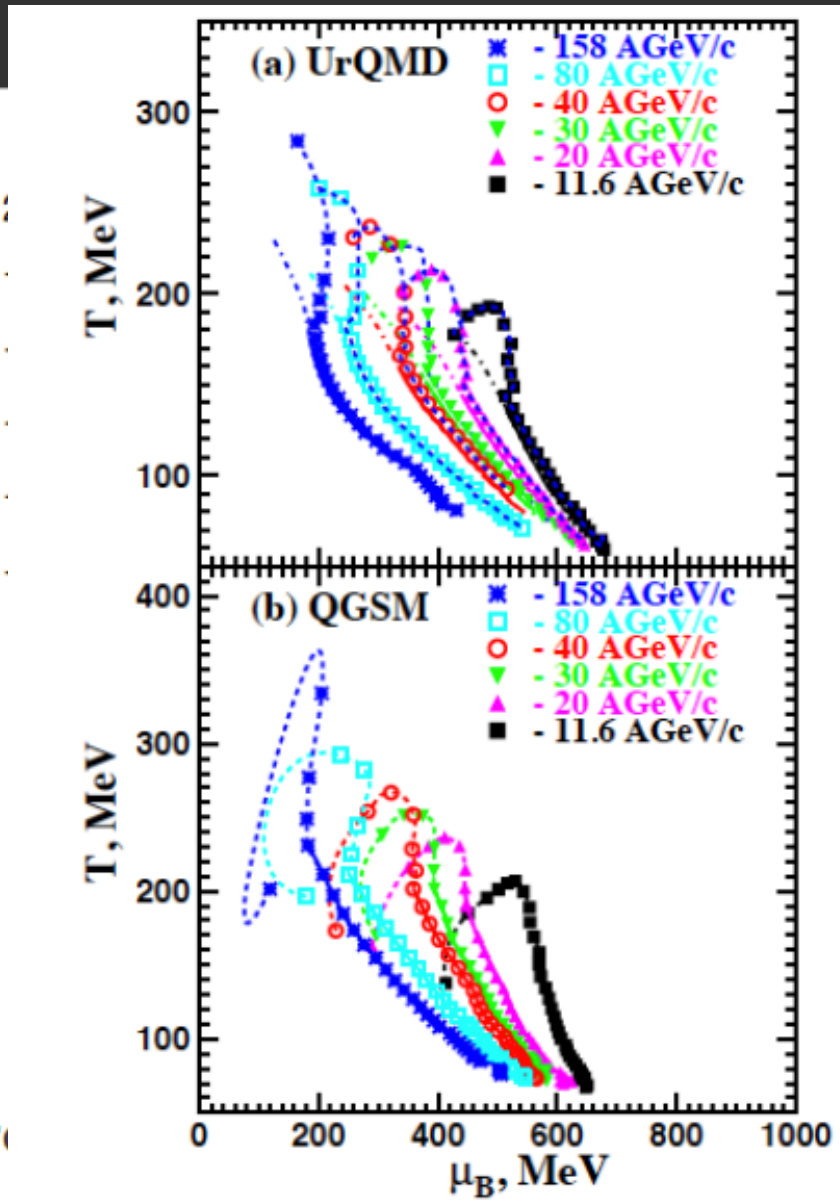

Freeze-out

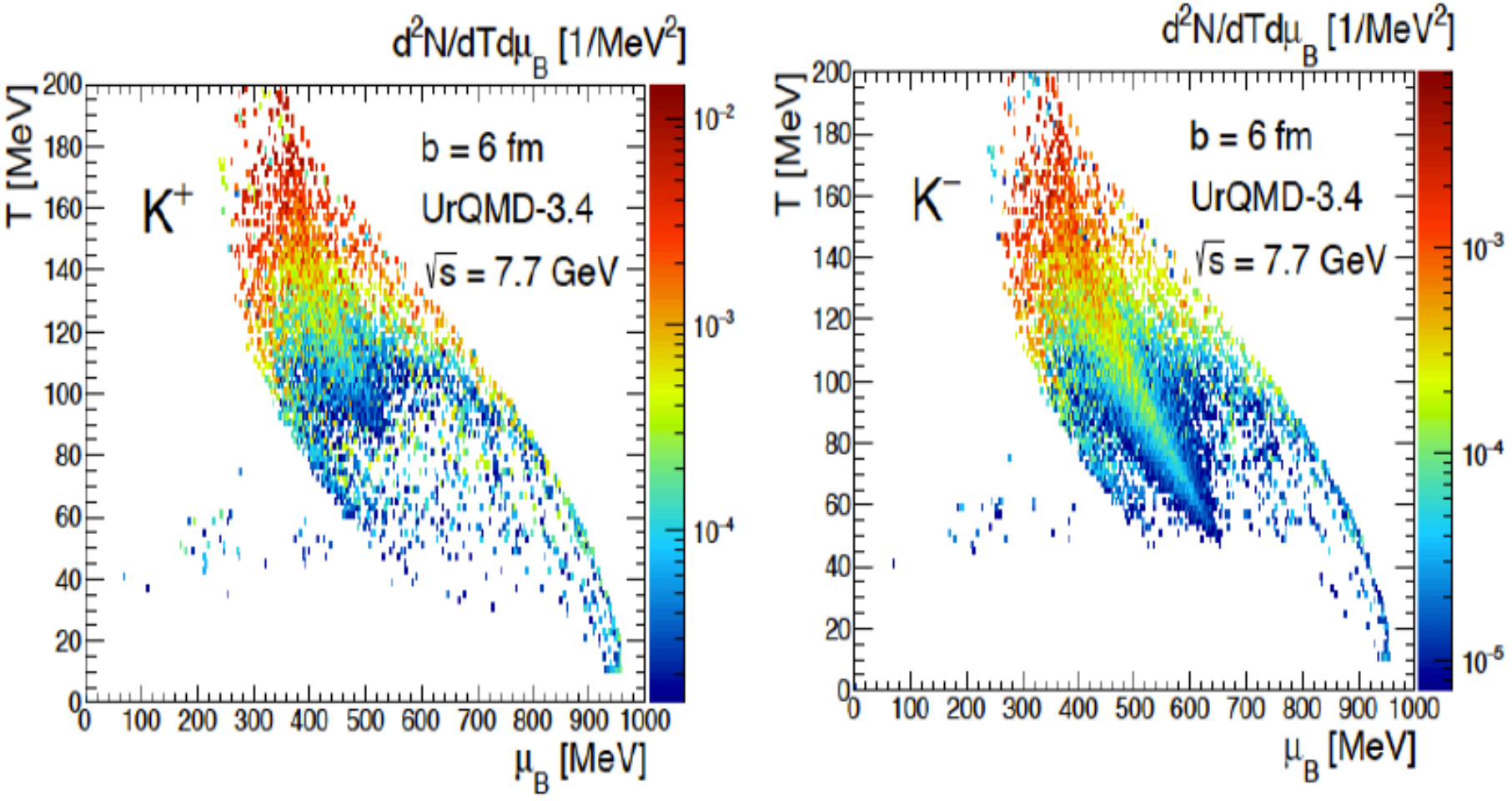

$d^2N/dTd\mu_B$ distribution of the final state hadrons over their formation point in (T, mu_B) plane at $\sqrt{s} = 7.7\ GeV,\ b = 6\ fm$.

Freeze-out

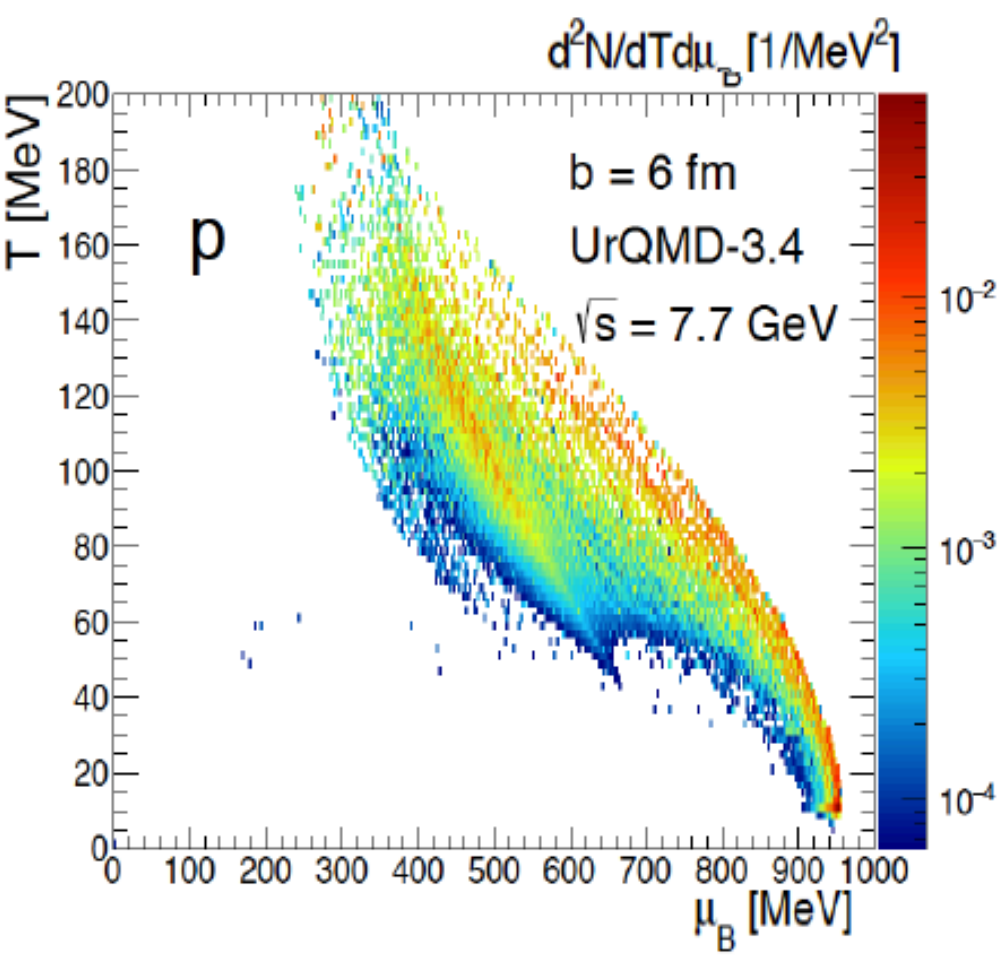

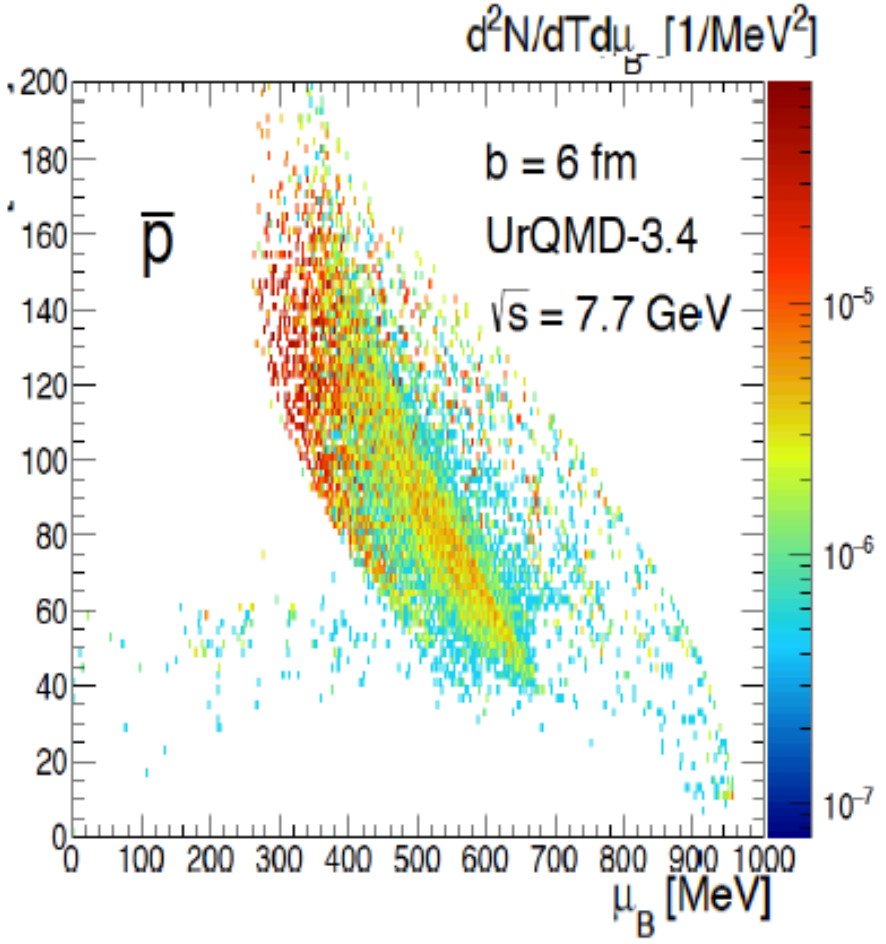

$d^2N/dTd\mu_B$ distribution of the final state hadrons over their formation point in (T, mu_B) plane at $\sqrt{s} = 7.7\ GeV,\ b = 6\ fm$.

Freeze-out

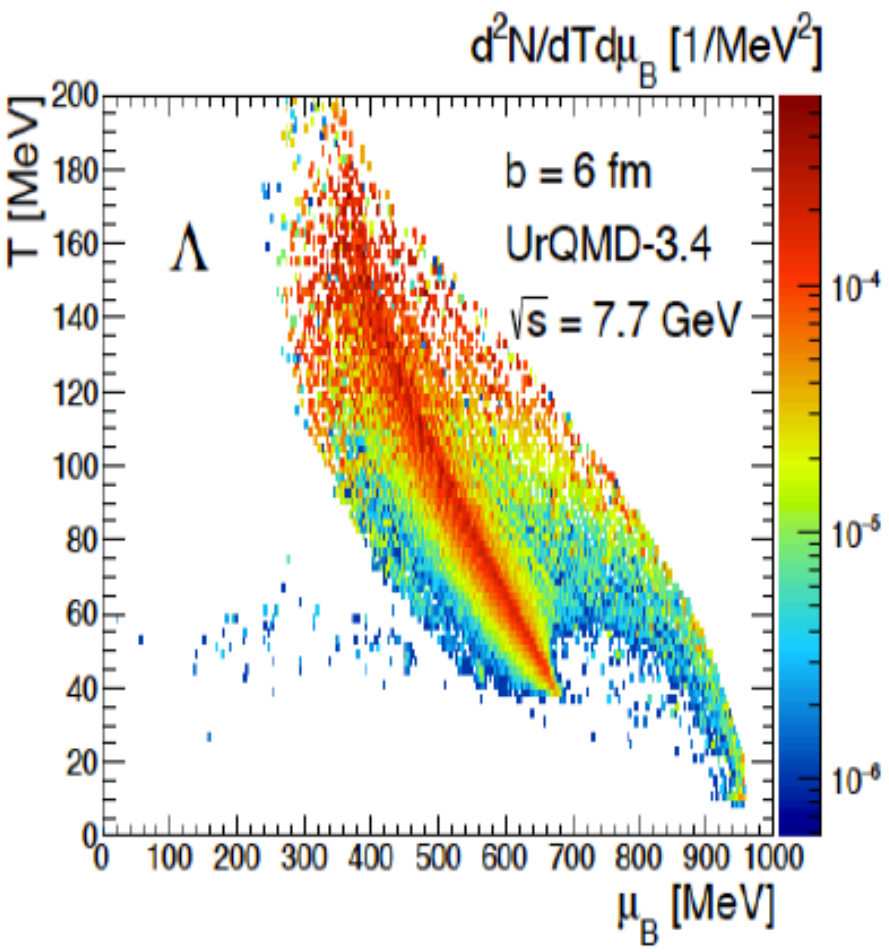

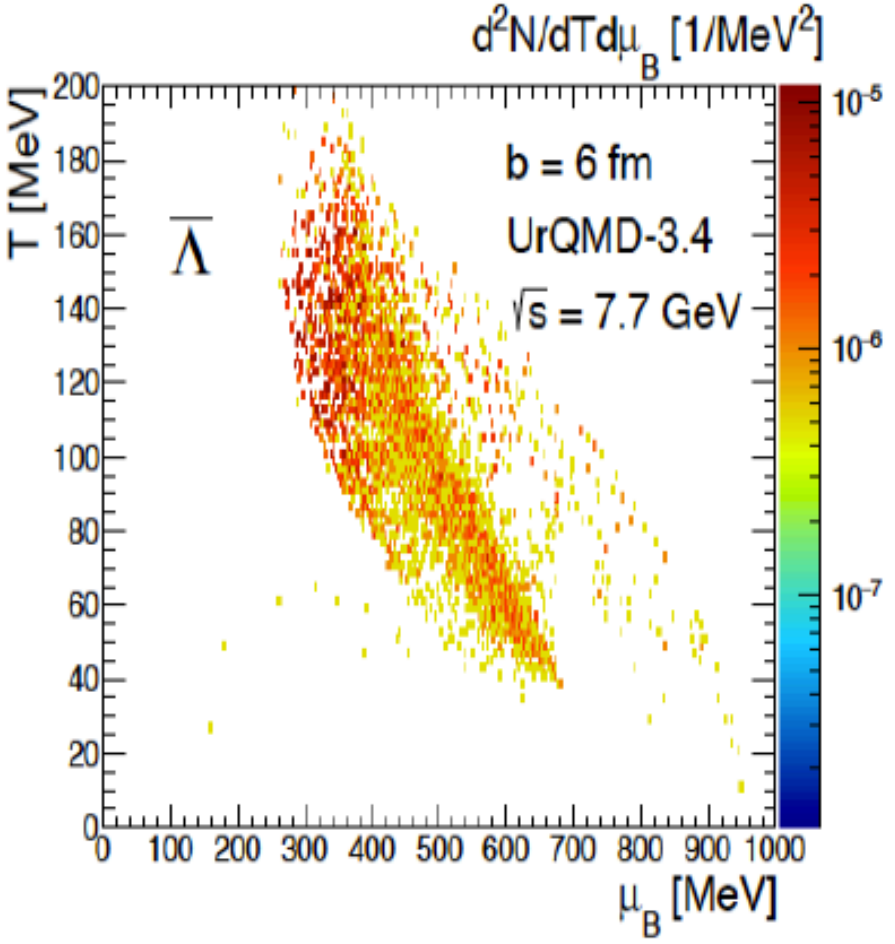

$d^2N/dTd\mu_B$ distribution of the final state hadrons over their formation point in (T, mu_B) plane at $\sqrt{s} = 7.7\ GeV,\ b = 6\ fm$.

Consequences of the different space-time freeze-out:
- Differences in yields in SM

L.Bravina et al, Springer Proceedings in Physics, vol. 250 (2020) p. 215

The difference between average freeze-out and freeze-out for particular species is very large

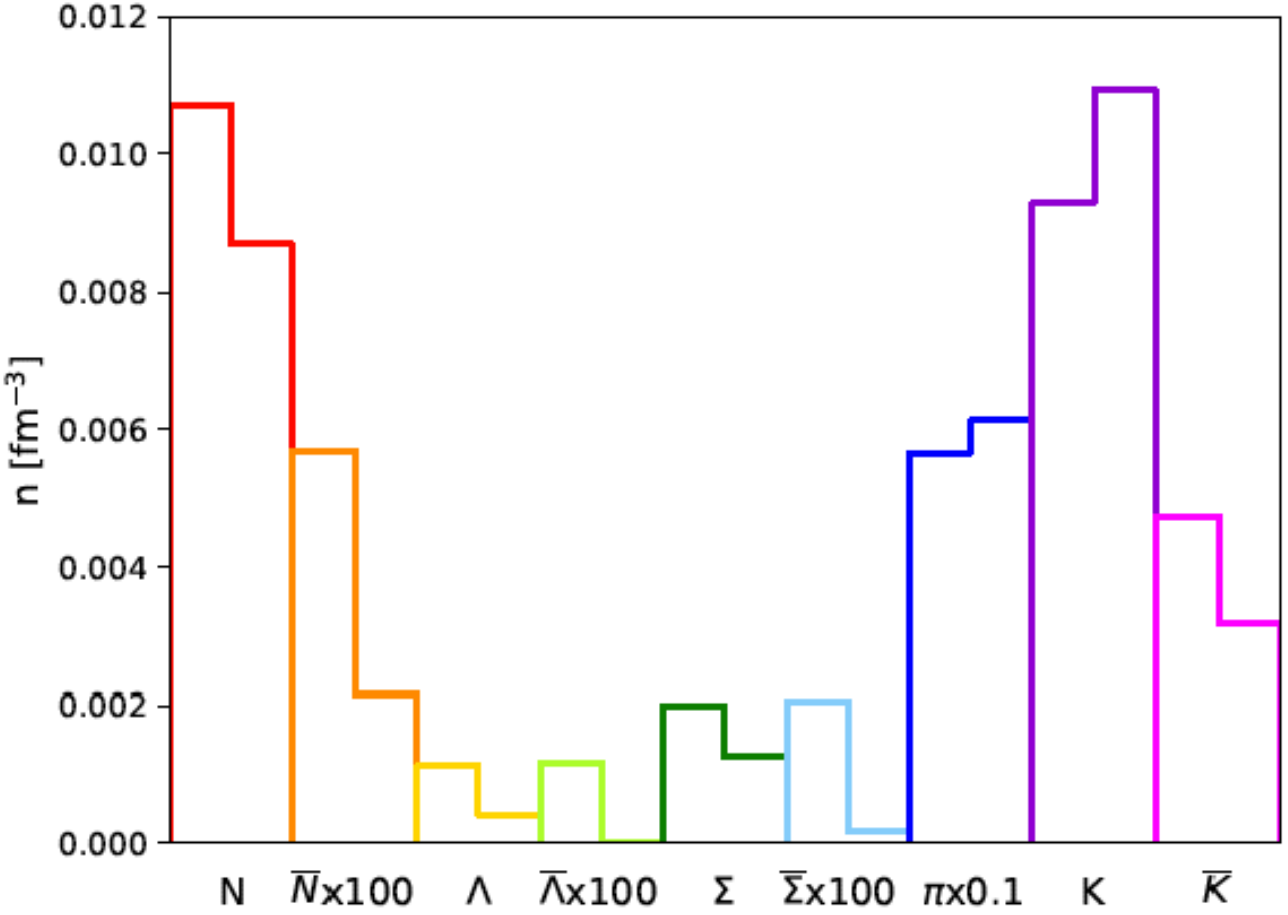

Figure 4: Particle densities at average freezeout coordinates of all particles (left column) and at freezeout coordinates of each particle type (right column) from statmodel; at average freezeout coordinates of all particles (star) and at freezeout coordinates of each particle type (pentagon) from UrQMD. E = 40A GeV.

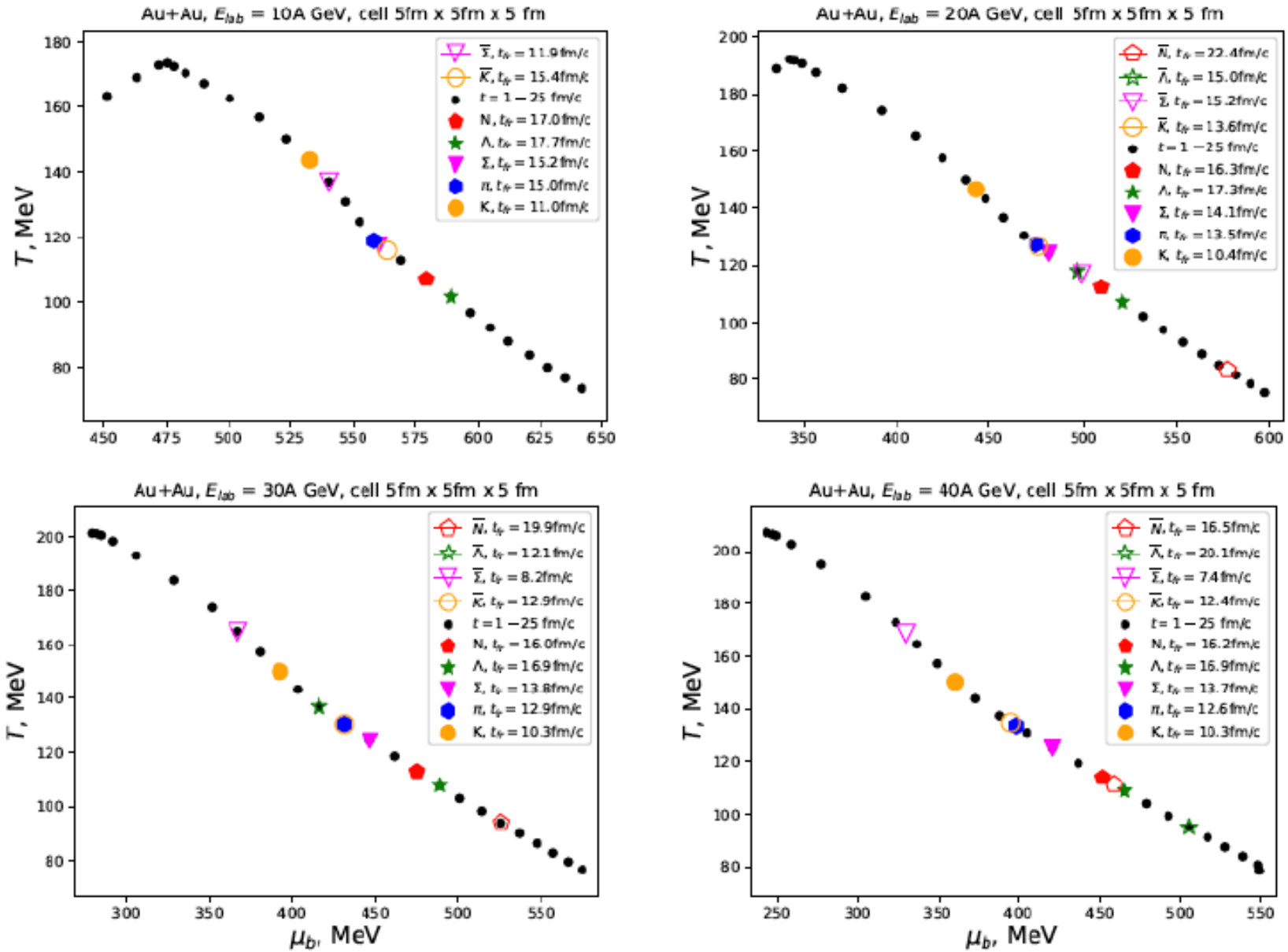

Figure 2: $T(\mu_B)$ in the central cell. Average freezeout times of different particles in the central cell are marked by colored markers.

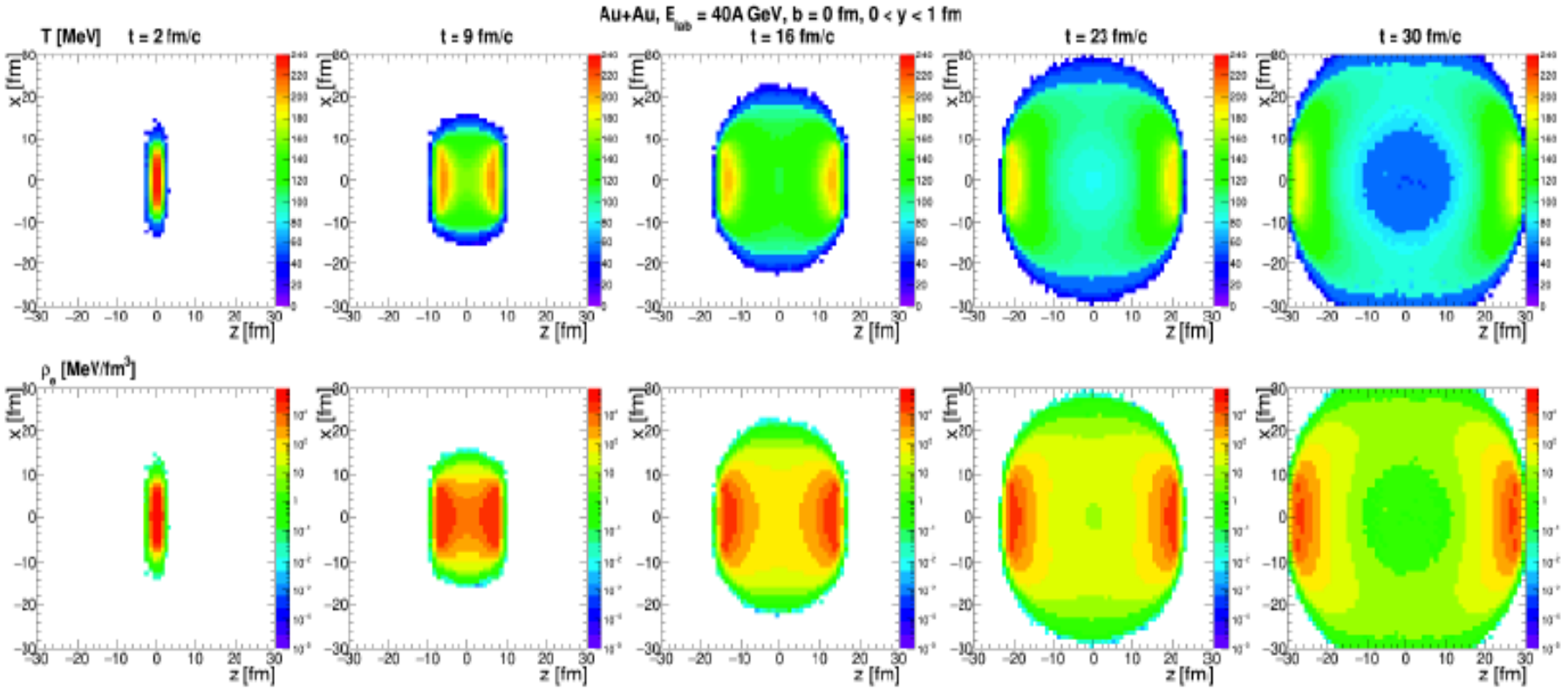

Figure 5: T and ε spatial distributions.

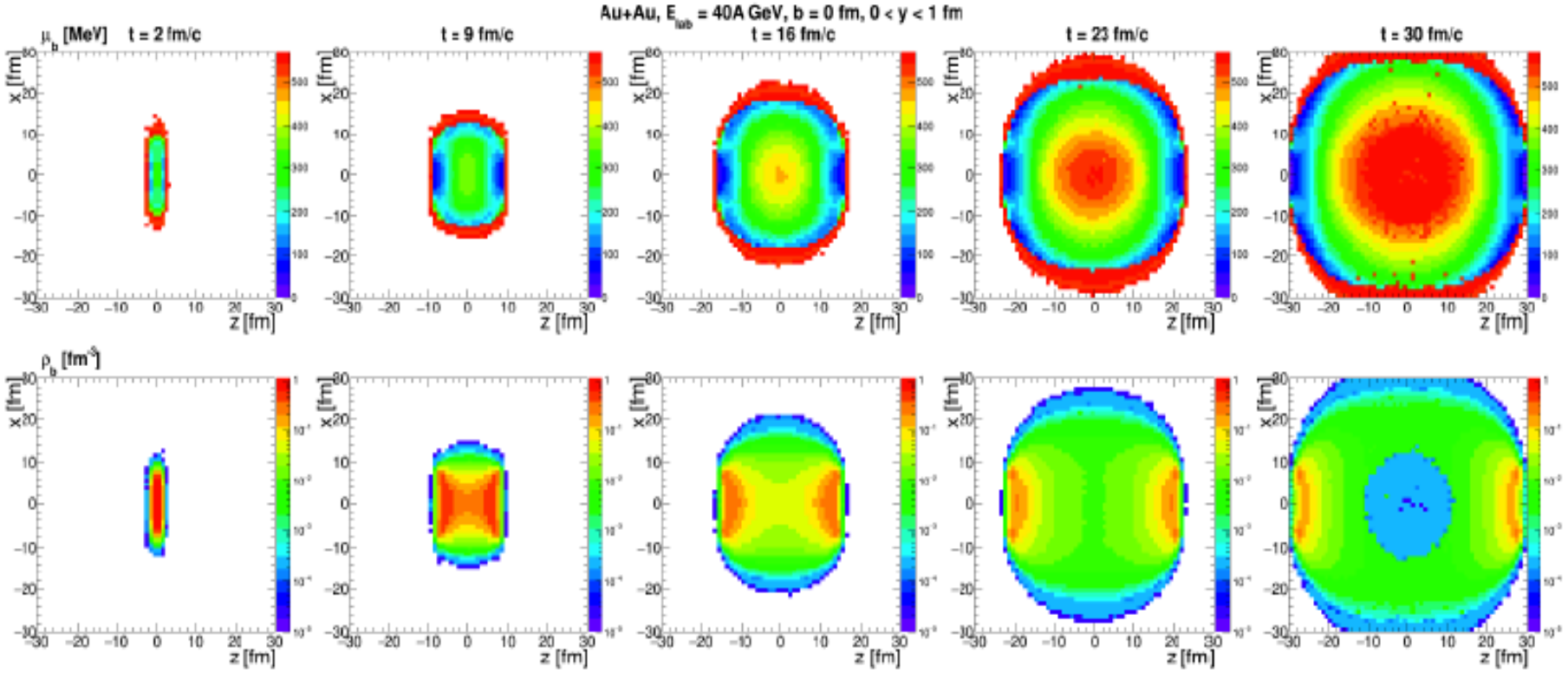

Figure 6: μ_b and ρ_b spatial distributions.

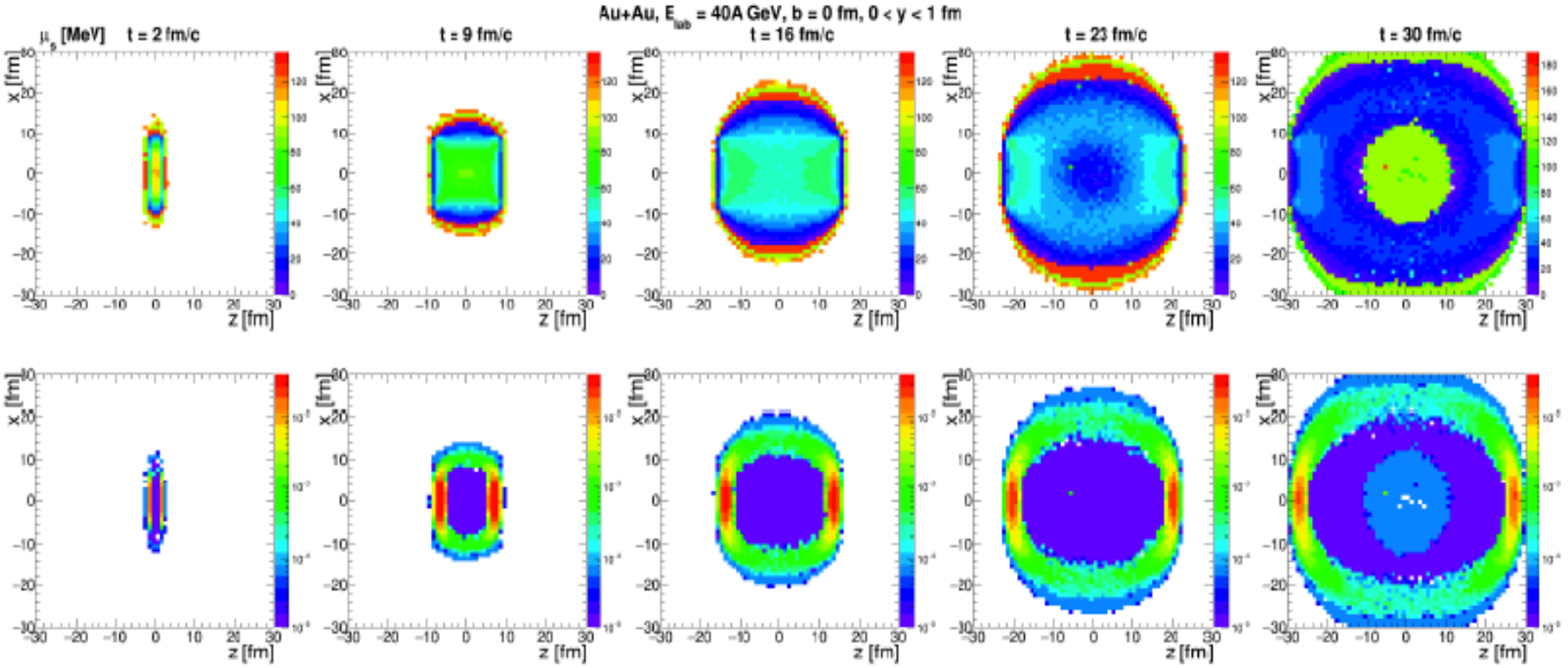

Figure 7: μ_s and ρ_s spatial distributions.

Conequences of the different space-time freeze-out:
- Directed flow

L.B. et al., Universe 5 (2019) 3, 69

Space distribution of Lambdas

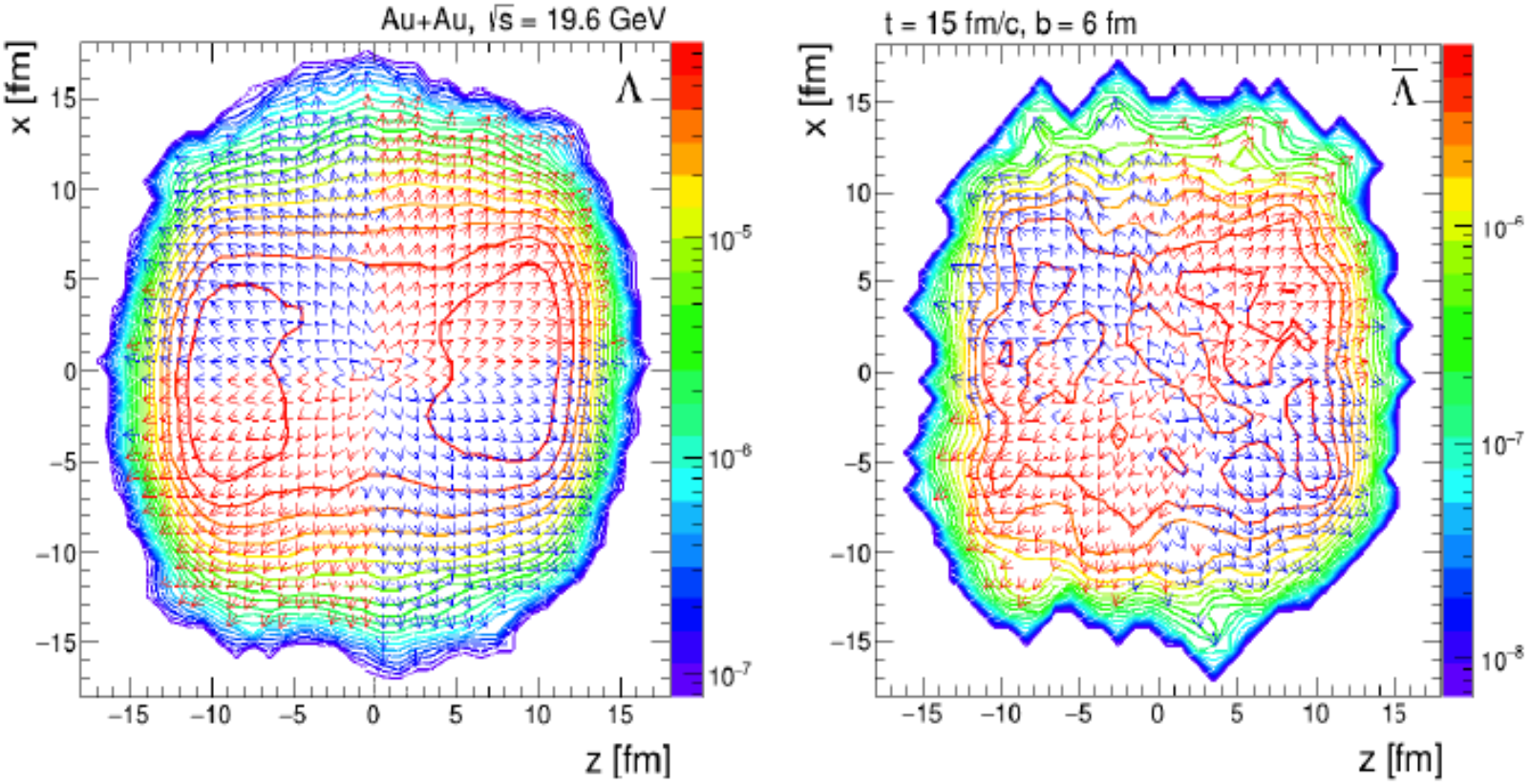

At $\sqrt{s} = 19.6 GeV$ Λ are mostly located near hot and dense regions and $\bar{\Lambda}$ are distributed more uniformly near system center.

Space distribution of Lambdas

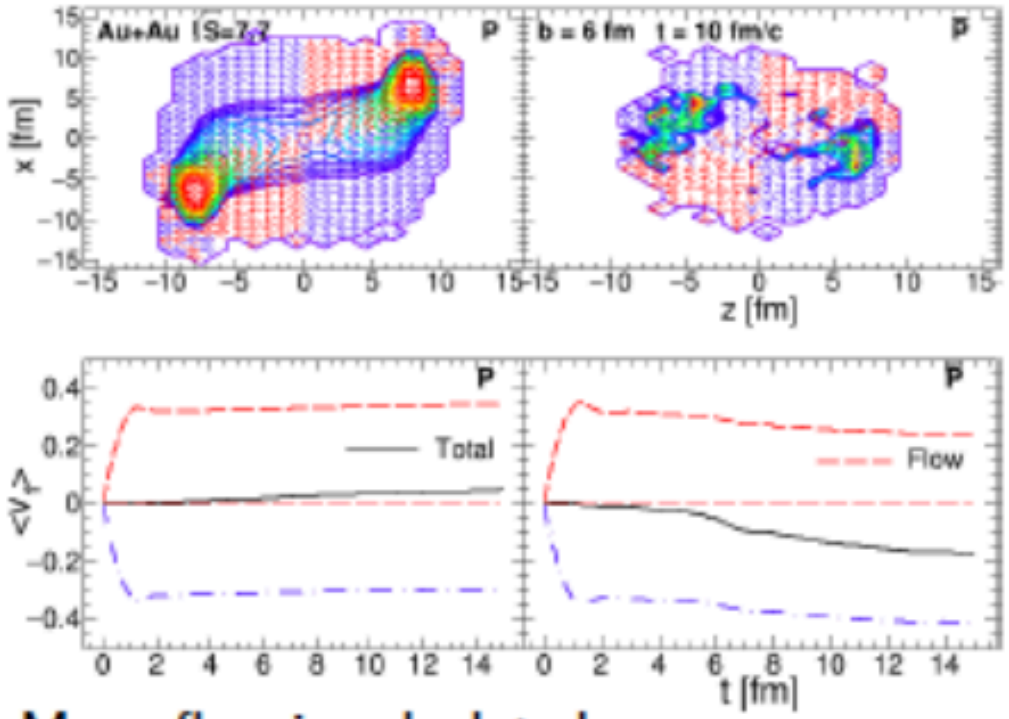

At low energies Λ and $\bar{\Lambda}$ are produced and emitted from the same regions as protons and antiprotons respectively. Λ's are concentrated also near hot and dense spectators, whereas $\bar{\Lambda}$'s are mostly produced in central region.

Mean flow is calculated as:

$$< v_1 >= \int sign(y) v_1(y) \frac{dN^{par}}{dy} dy \Big/ \int \frac{dN^{par}}{dy} dy$$

Collective velocities are shown on the picture to demonstrate that particles which have positive product of velocities $v_x v_z$ produce normal component of flow and particles with $v_x v_z < 0$ produce anti-flow component of directed flow. [Bravina et al, EPJ Web of Conferences 191, 05004 (2018)]

Directed flow for Lambdas and kaons

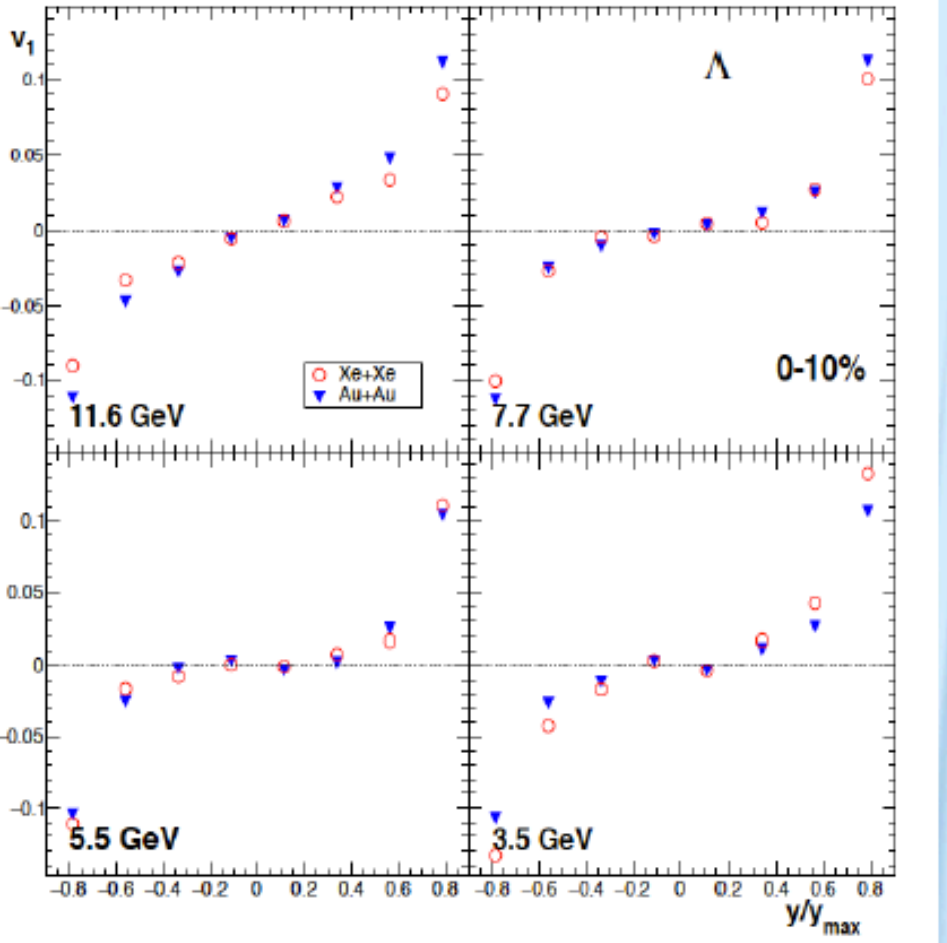

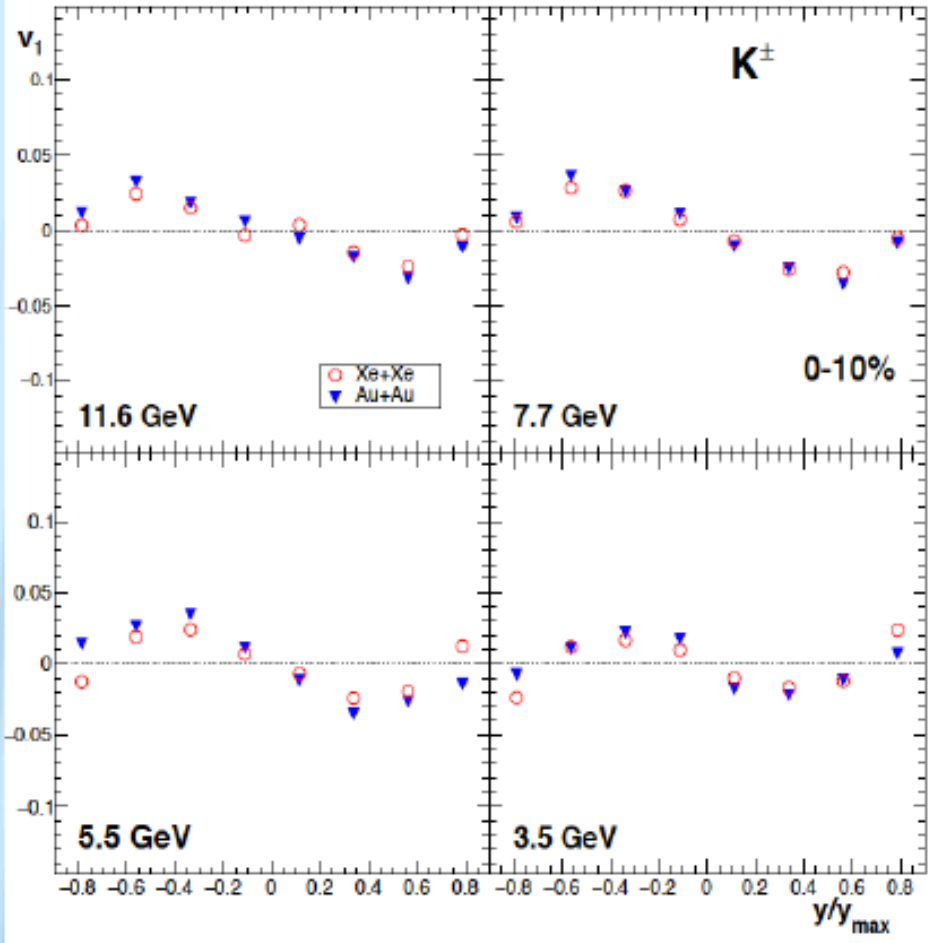

V_1 for Λ changes sign at midrapidity with decreasing collision energy, whereas V_1 for kaons has negative slope (antiflow)

Different slopes of different particles: URQMD and Data

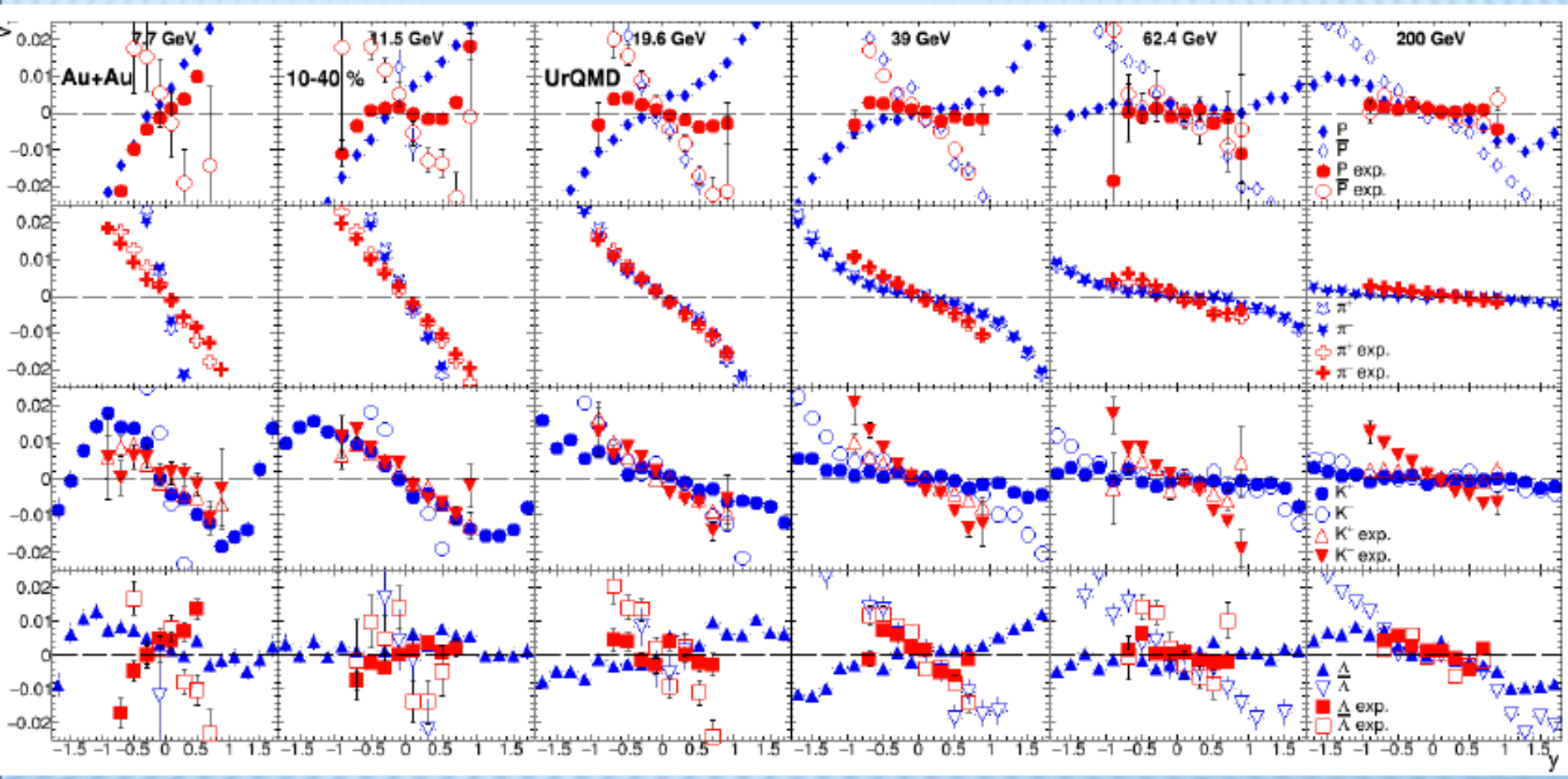

Consequences of the different space-time freeze-out:
- Difference in Polarization for lambdas and antilambdas

O.VITIUK ET AL SPRINGER PROCEEDINGS IN PHYSICS, VOL. 250 (2020) P. 429

O.Vitiuk, L.B., E.Zabrodin, PLB 803 (2020) 135298

Motivation

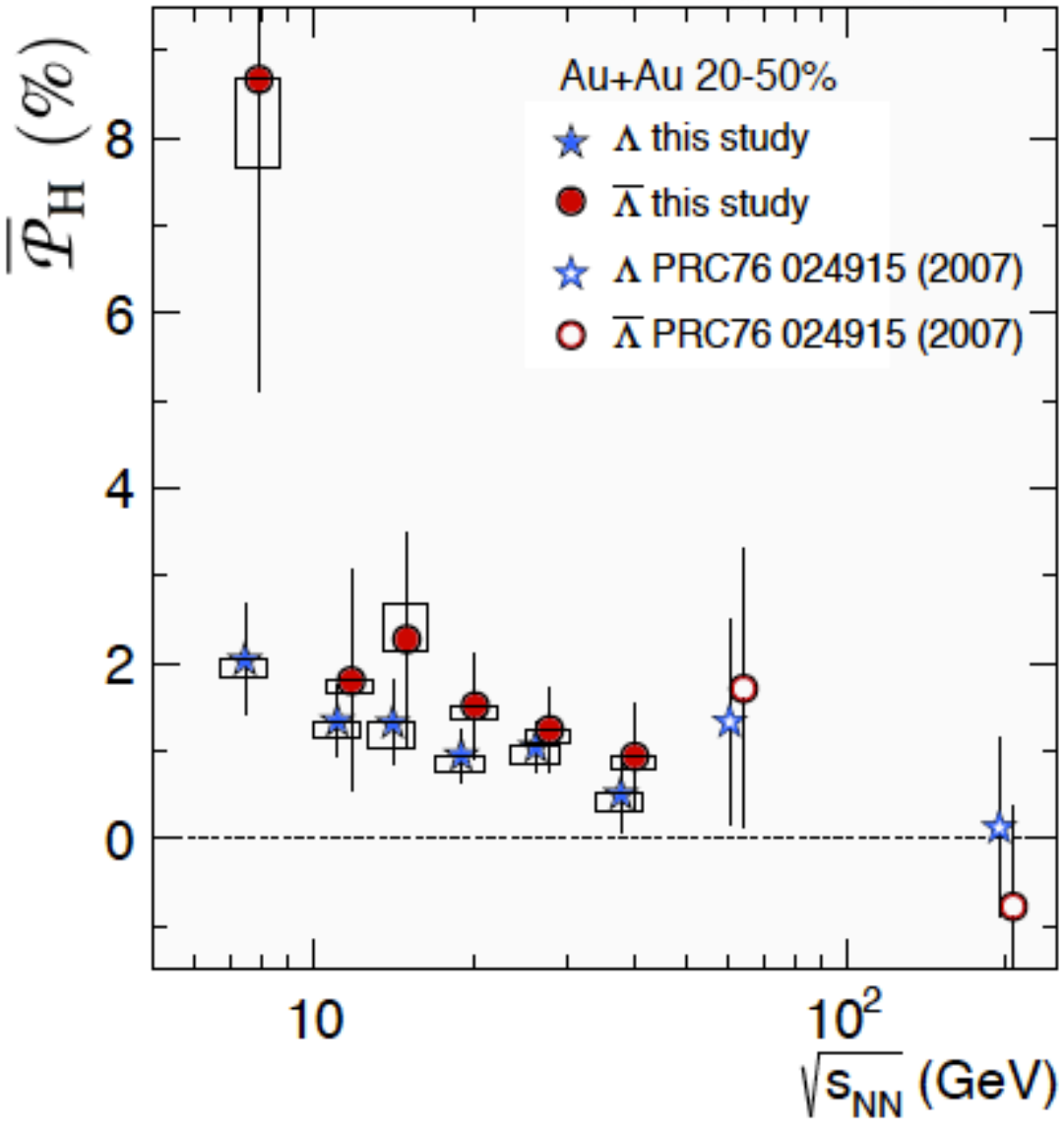

"The discovery of global Lambda polarization in non-central heavy ion collisions opens new directions in the study of the hottest, least viscous - and now, most vortical - fluid ever produced in the laboratory."

STAR Collaboration, Nature 548 (2017) 62

Freeze-out of hyperons

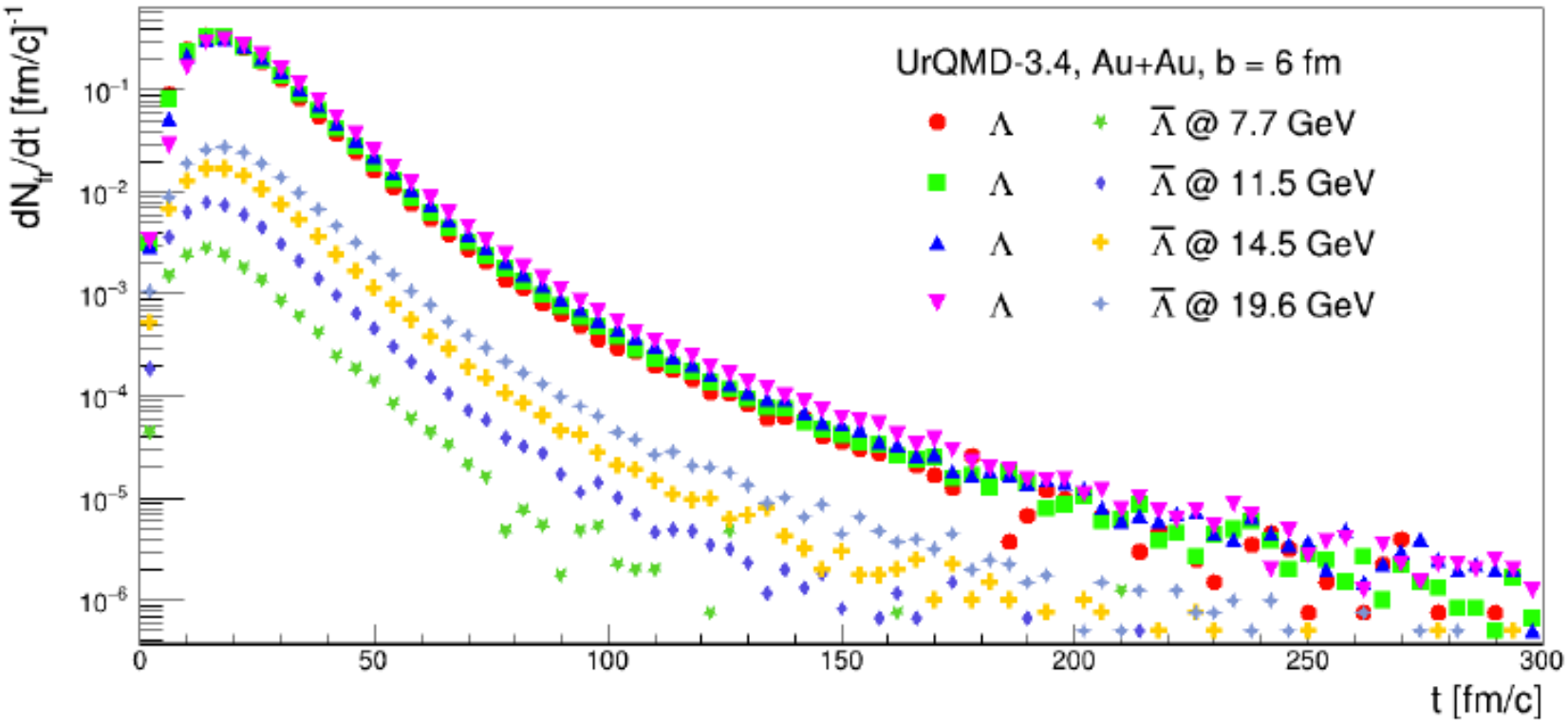

Λ's and $\bar{\Lambda}$'s with $|y| < 1$ and $0.2 < p_t < 3$ GeV/c were analyzed.

$\sqrt{s}$ [GeV]	7.7	11.5	14.5	19.6
Mean freeze-out time Λ [fm/c]	21.3009	21.9568	23.066	24.3462
Mean freeze-out time $\bar{\Lambda}$ [fm/c]	19.7806	21.0302	21.959	23.1288

Thermal vorticity in reaction plane

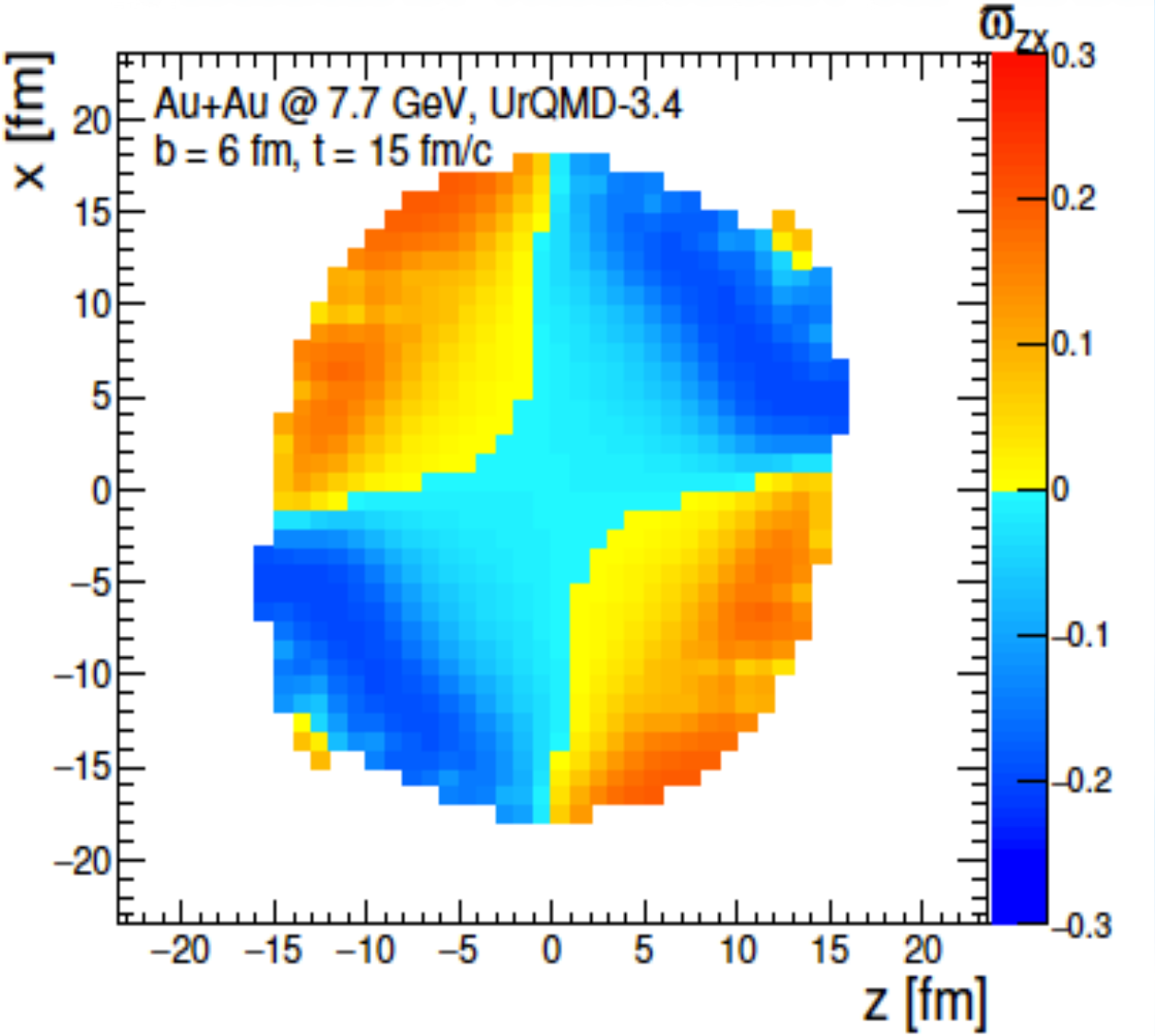

Thermal vorticity component ω_{zx} has quadruple structure in the reaction plane. The value of ω_{zx} decreases with the expansion of the system. The first and third quadrants are associated with a central region with a slight negative vorticity. This connecting part becomes smaller as the energy of the colliding nuclei increases.

Proper Temperature

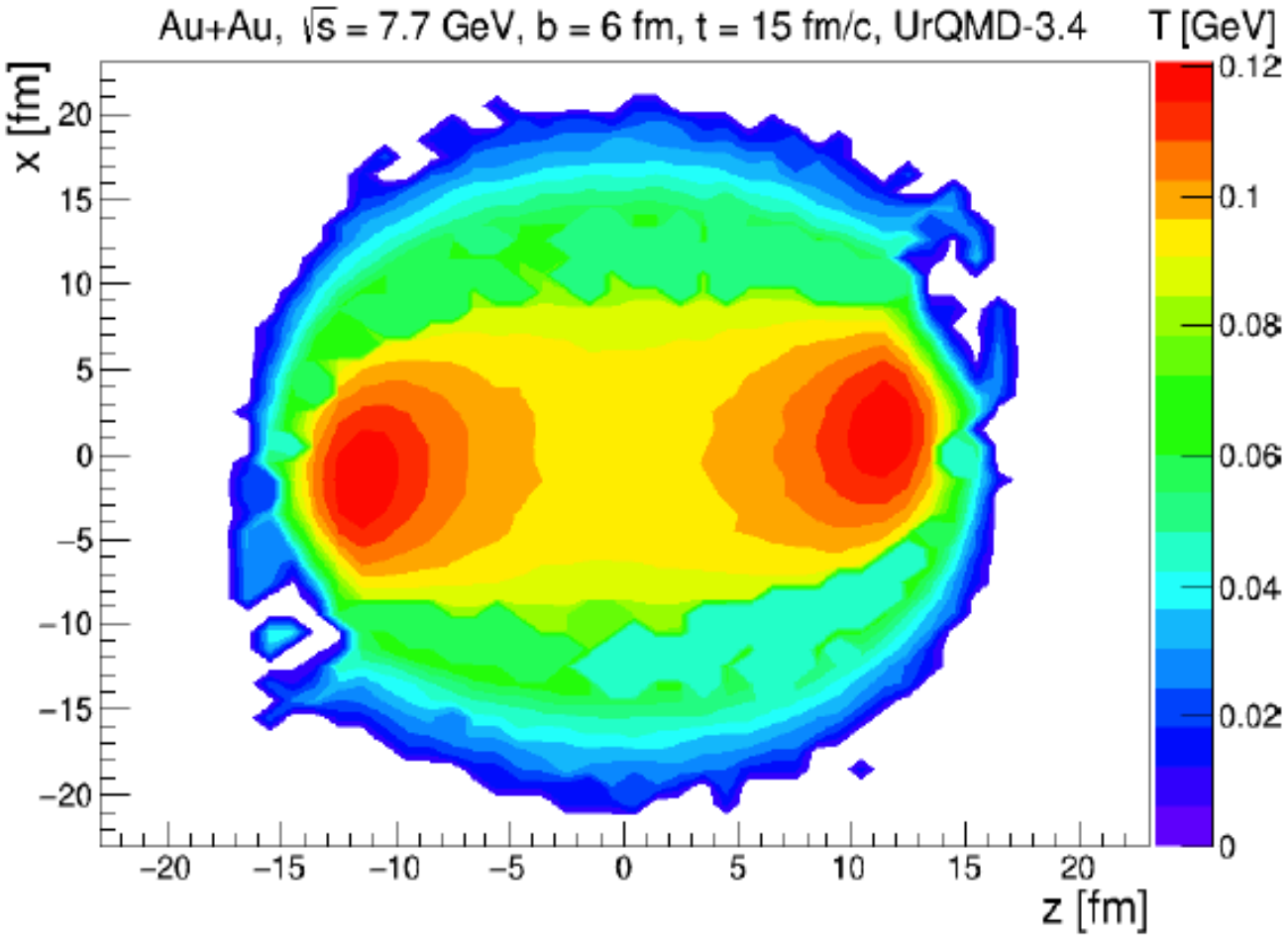

Temperature extracted with statistical model is not uniform. There are two main regions. More hot regions with T $\simeq 100 MeV$ are connected to dense spectators. The other part is related to fireball with temperature $\simeq 60 MeV$.

Spatial distribution of Λ and anti-Λ

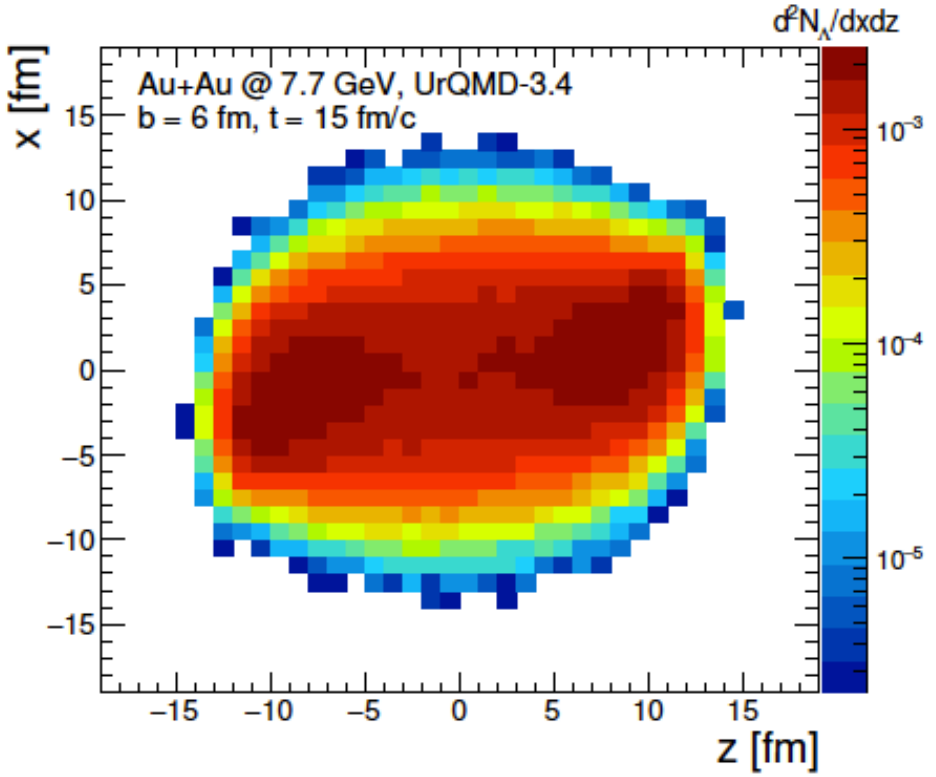

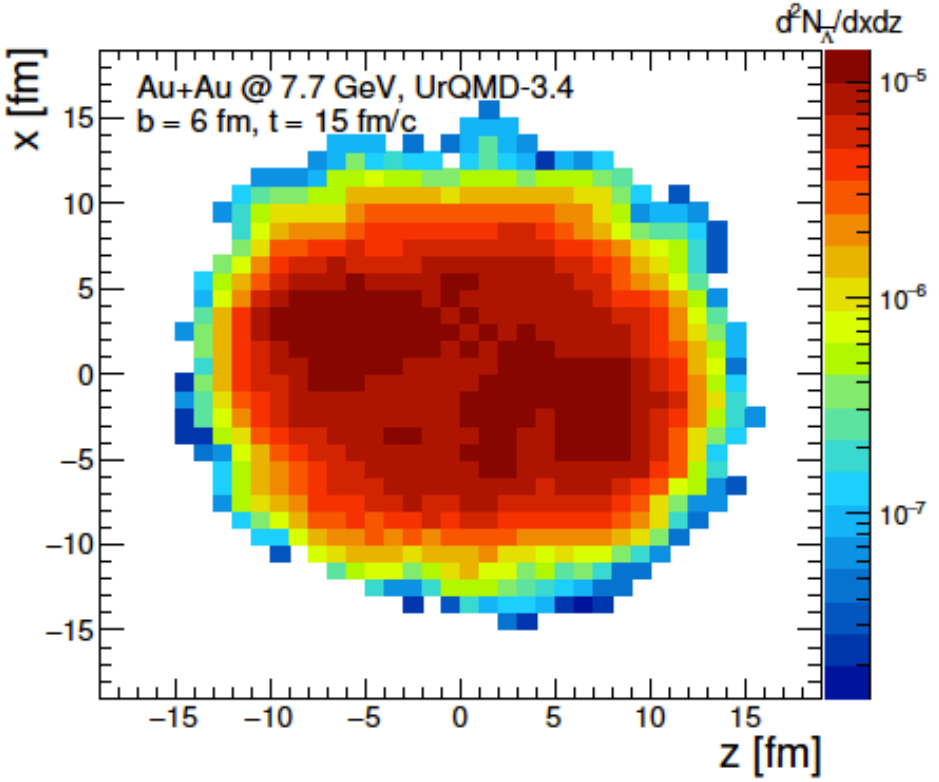

At $\sqrt{s} = 7.7\ GeV$ Λ are mostly located near hot and dense regions and $\bar{\Lambda}$ are distributed more uniformly near system center.

Polarization of Λ and anti-Λ

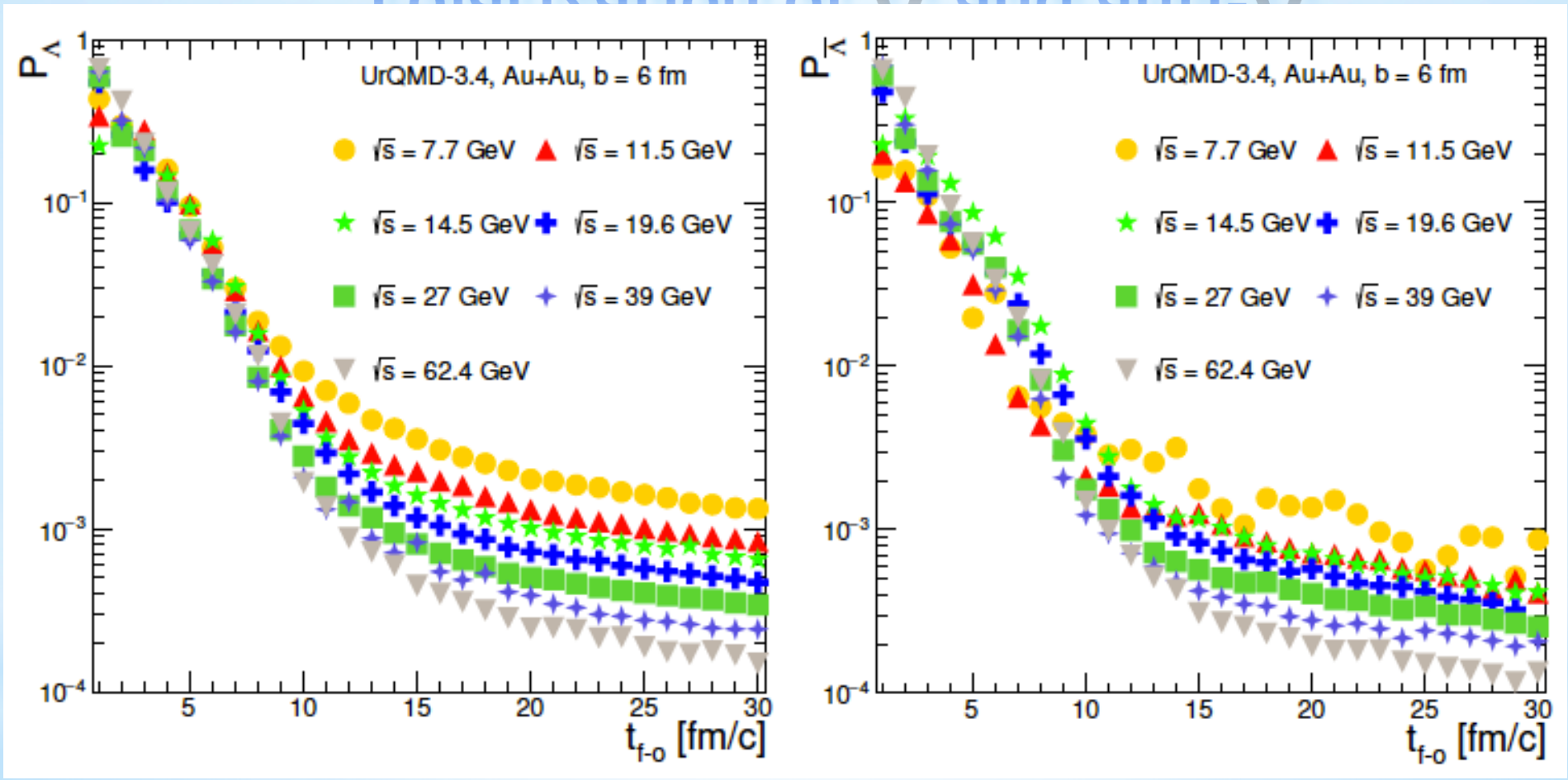

The polarization of both hyperons decreases with time. In the early stages, Lambdas form mainly in hot and dense areas with high polarization. The polarization of the (anti-) Lambdas formed after t = 10 fm /c is close to zero.

Energy dependence of global polarization of Λ and anti-Λ

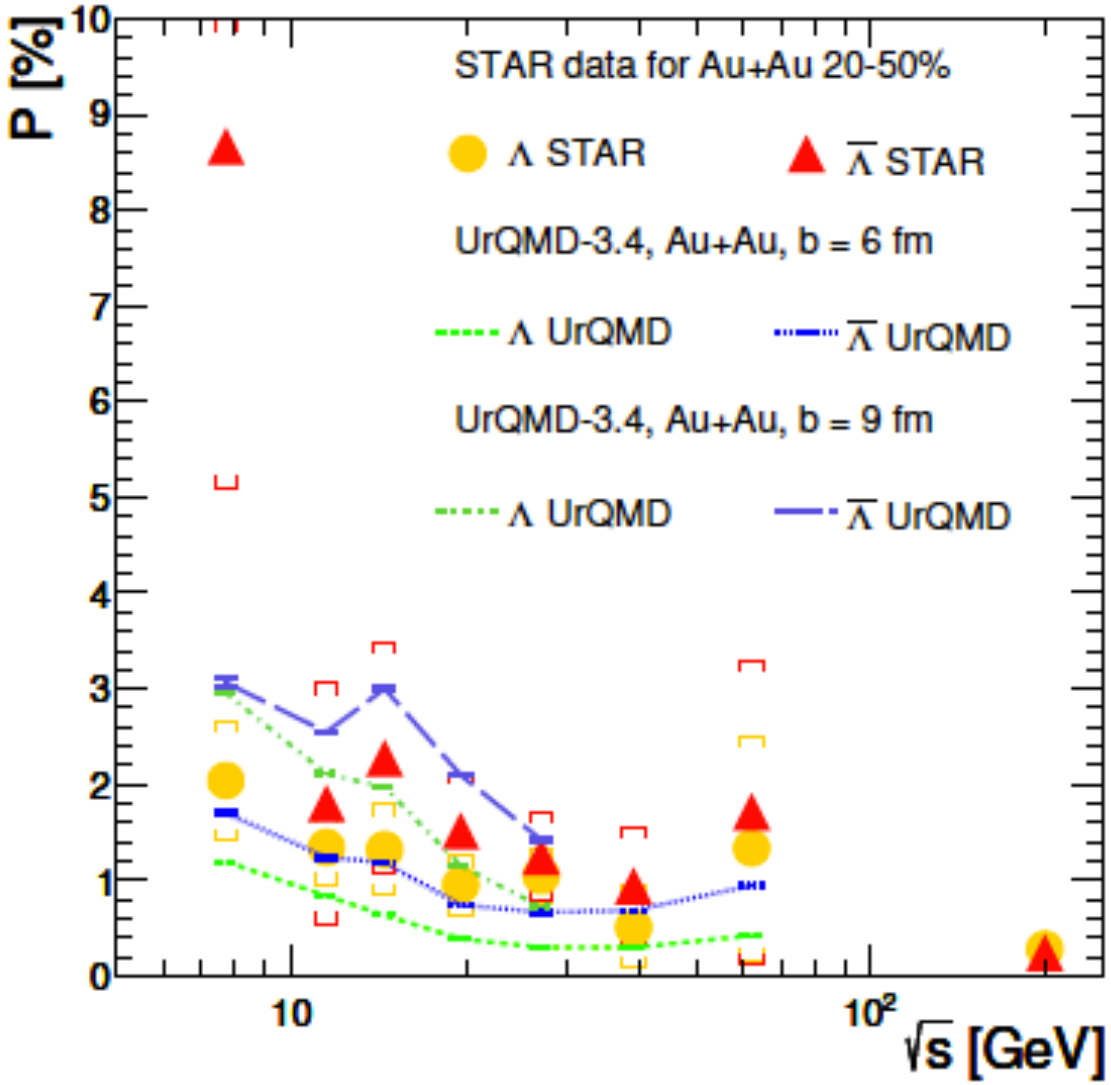

The difference between the global polarization of both hyperons is due to

(1) different space-time distributions of Lambdas and anti-Lambdas and

(2) different thermal vorticity in the freeze-out regions of both hyperons.

Data: STAR Collaboration, PRC 98 (2018) 014910

Comparison with other models

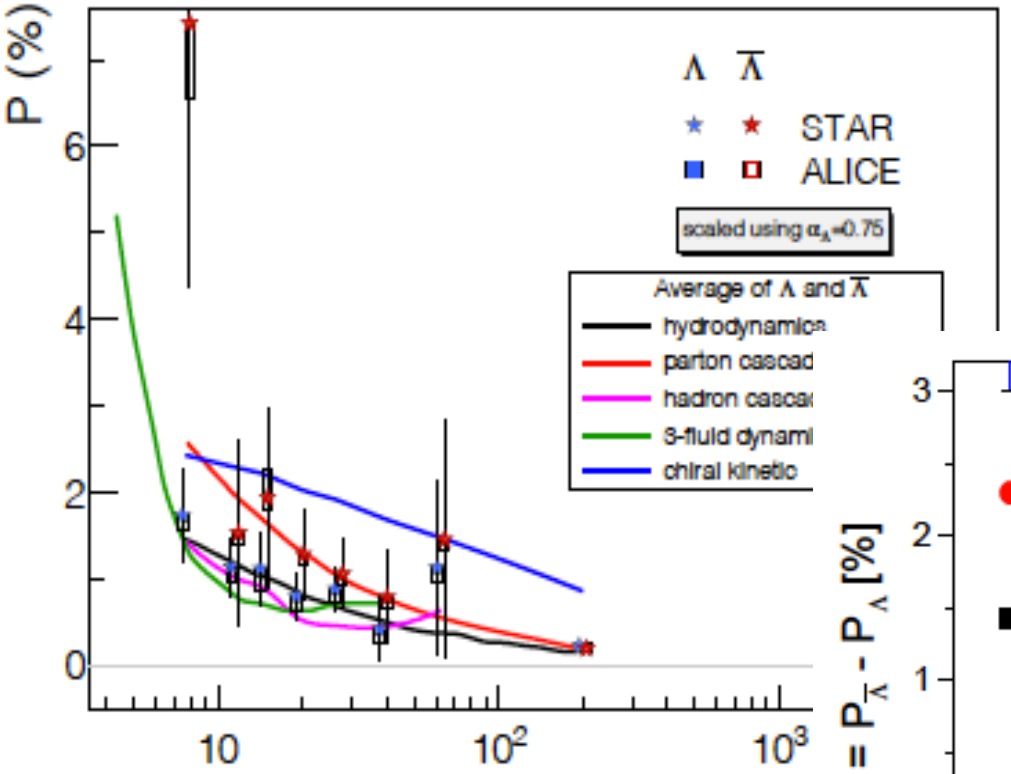

Y.Xie, G.Chen, L.P.Csernai, EPJC 81 (2021) 12

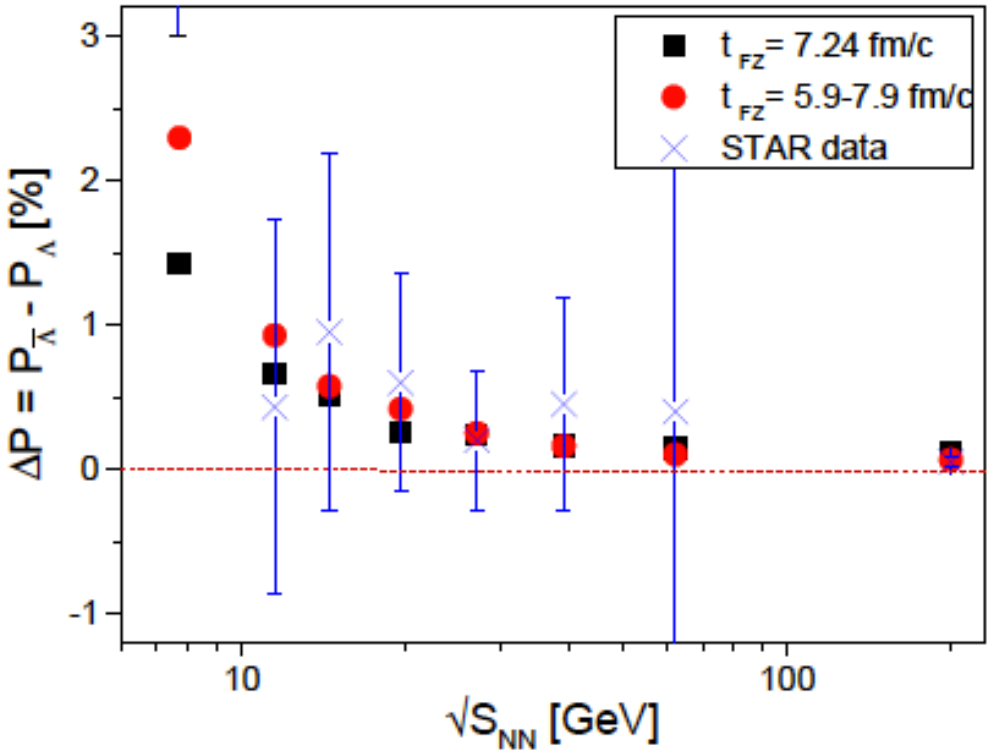

F.Becattini and M.A.Lisa, Ann. Rev. Nucl. Part. Sci. 70 (2020) 395

IV. Cross-over between phase and space freeze-out (in collaboration with Yu. Sinyukov et al)

Y. Kravchenko(1), L. Bravina(2), E. Khyzhniak(3), G. Nigmatkulov(3), Y. Sinyukov(4), E. Zabrodin(2)

SPATIOTEMPORAL STRUCTURE OF THE PION EMISSION IN AU+AU COLLISIONS AT $\sqrt{s_{NN}}$ = 19.6 GEV IN THE URQMD MODEL

Physica Scripta 96 (2021) 10, 104002

Correlation functions

- Charged pions were considered
- Correlation functions built as ratio of distributions with and without weight:

$$C(q_{long}, q_{out}, q_{side}) = \frac{A(q_{long}, q_{out}, q_{side}; w)}{B(q_{long}, q_{out}, q_{side})}$$

$$w = 1 + cos(q \cdot r)$$

q - pair relative 4-momentum,
r - pair relative 4-coordinates

$q_{long}, q_{out}, q_{side}$ - in Bertsch-Pratt parametrization

- Analysed independently pion pairs with $k_T = \frac{|\vec{p}_{T1} + \vec{p}_{T2}|}{2}$ in ranges:

[0.05,0.15], [0.15,0.25], [0.25,0.35], [0.35,0.45], [0.45,0.55], [0.55,0.65], [0.65,0.75] GeV/c

The following transformations of relative momentum were applied:

- Lorentz boost into the system of the pair`s center of mass along the Z axis.
- Coordinate rotation according to Bertsch-Pratt parametrization:
  - Long direction - parallel to the beam (z axis)
  - Out direction - parallel to $\overrightarrow{k_T}$
  - Side direction - perpendicular to long and out

Correlation function fit

$$C(q_{long}, q_{out}, q_{side}) = 1 + \lambda \cdot e^{-R^2_{long}\, q^2_{long} - R^2_{out}\, q^2_{out} - R^2_{side}\, q^2_{side}}$$

m_T dependence of correlation radii

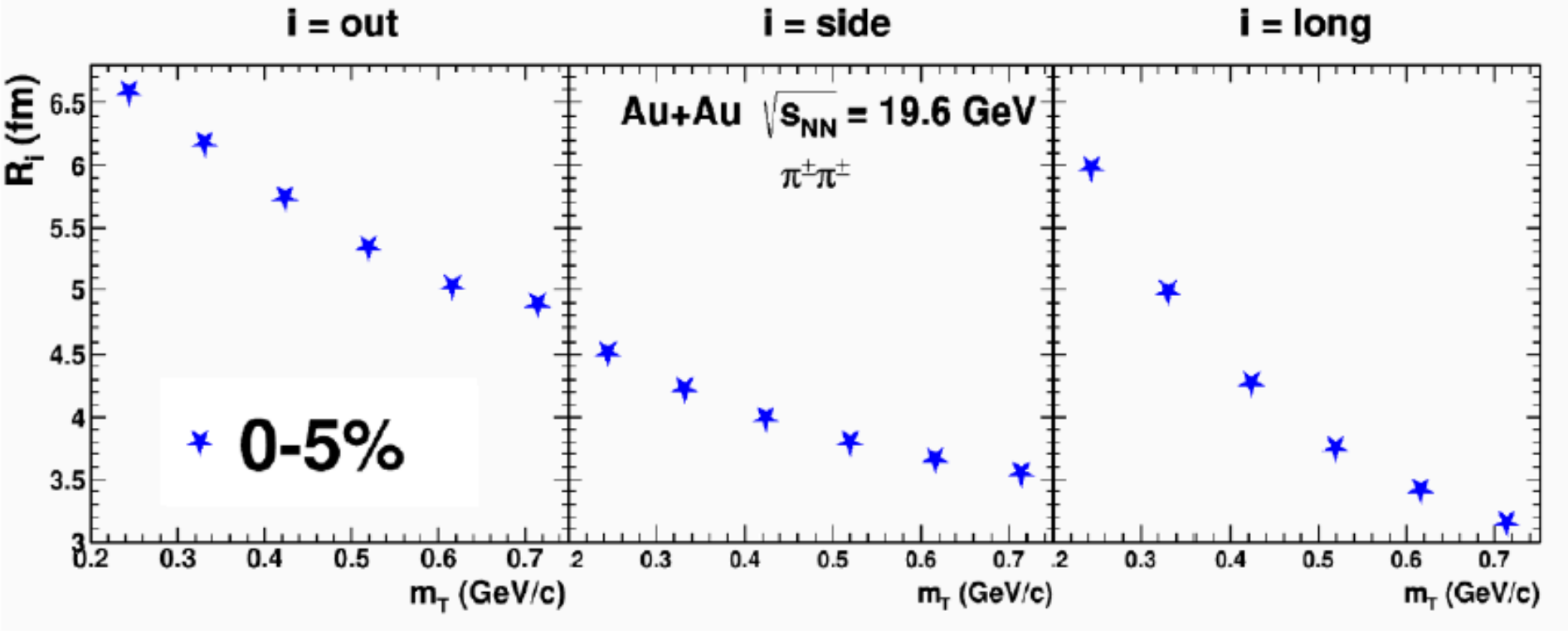

Obtaining τ from R_{long} fit

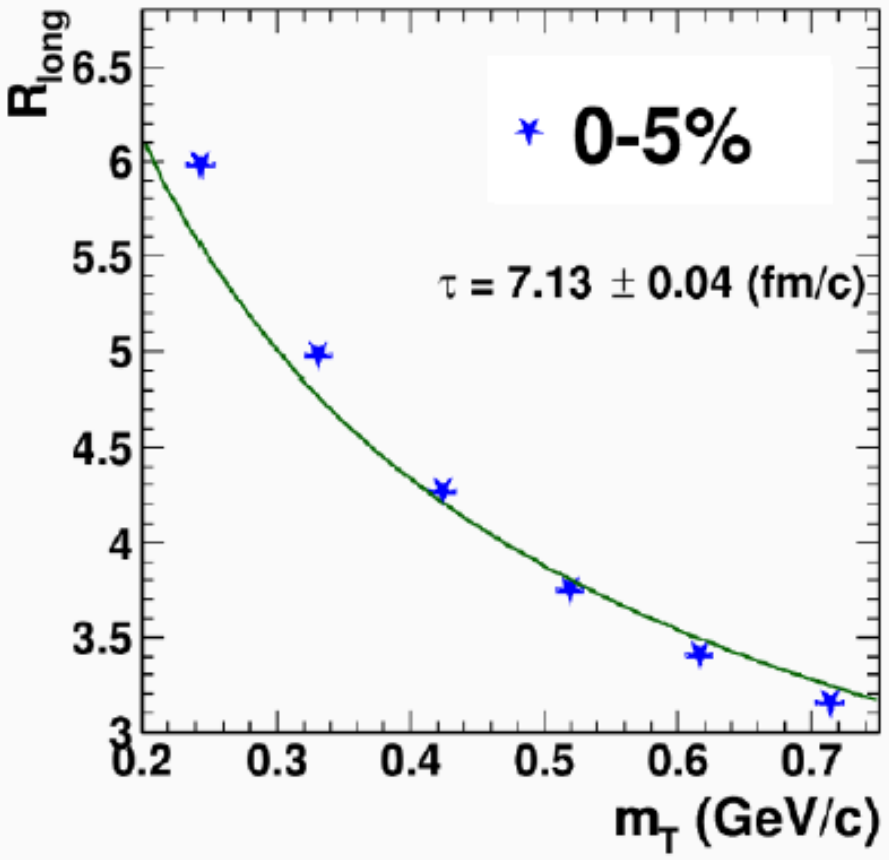

Dependency of R_{long} fitted with:

$$R_{long} = \tau \cdot \sqrt{\frac{T}{m_T}}$$

$$\tau = 7.13 \pm 0.04\ fm/c$$

Emission function distribution

The second approach is based on a direct analysis of the last collision points. In UrQMD full information about last collision points is available, that allows studying the spatiotemporal structure of emission function straightforwardly.

Considered distribution of π^+ kinetic freeze-out:

$$\frac{dN^2}{r_T \cdot d\tau dr_T}$$

Where:

$$\tau = \sqrt{t^2 - z^2}$$

$$r_T = \sqrt{r_x^2 + r_y^2}$$

With the following cuts:

Time-space rapidity: $$|\frac{1}{2} \cdot ln\frac{t+z}{t-z}| < 0.5$$

Momentum rapidity: $$|\frac{1}{2} \cdot ln\frac{E+p_z}{E-p_z}| < 0.5$$

Distributions built separately for p_T in ranges:

[0,0.1], [0.1,0.2], [0.2,0.3], [0.3,0.4], [0.4,0.5], [0.5,0.6], [0.6,0.7], [0.7,0.8], [0.8,0.9]

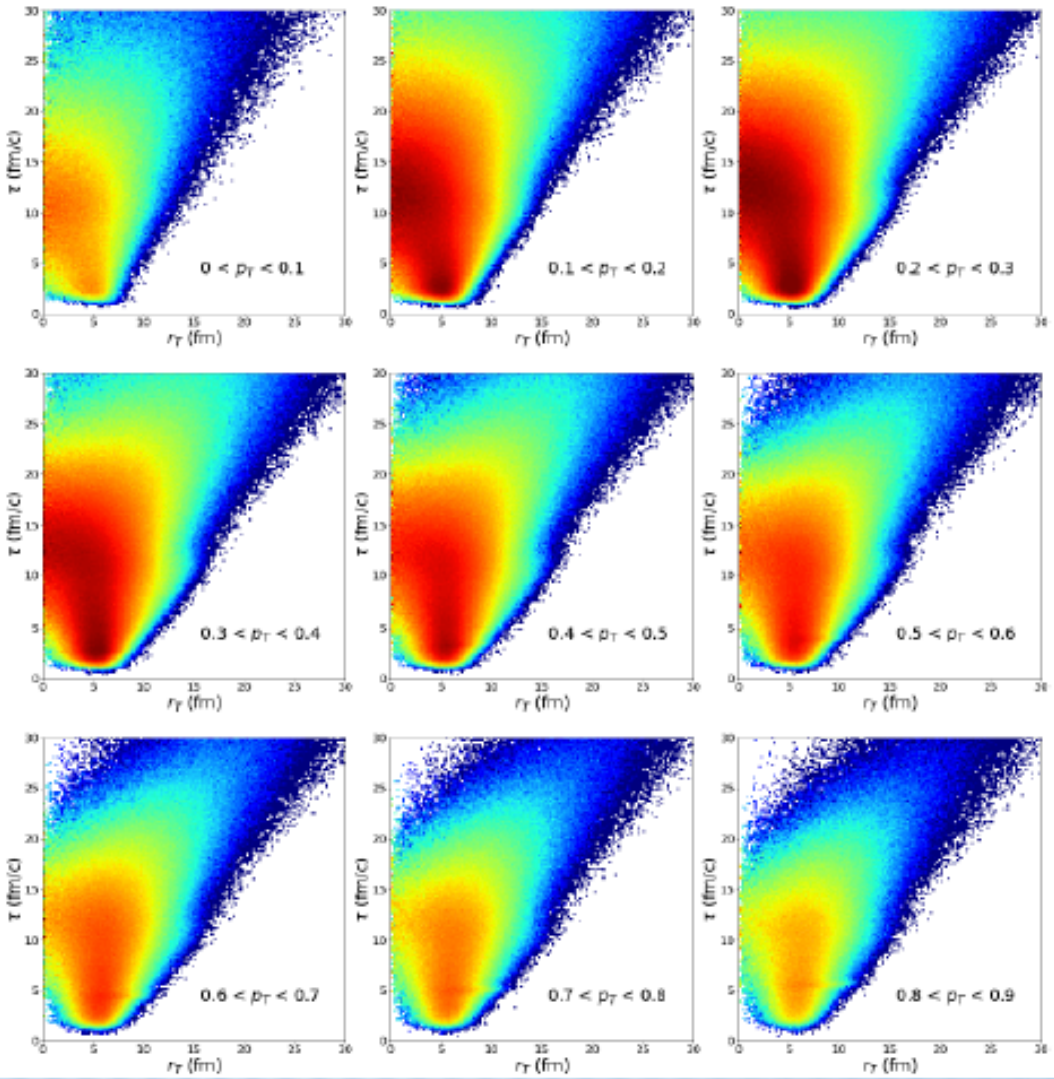
$0 < p_T < 0.1$
$0.1 < p_T < 0.2$
$0.2 < p_T < 0.3$
$0.3 < p_T < 0.4$
$0.4 < p_T < 0.5$
$0.5 < p_T < 0.6$
$0.6 < p_T < 0.7$
$0.7 < p_T < 0.8$
$0.8 < p_T < 0.9$
r_T (fm)
τ (fm/c)
$\frac{dN^2}{r_T \cdot d\tau dr_T}$

To the accordance with asymptotic formulas, high-p_T will be considered further.

In the area of $p_T > 0.4$ GeV/c maximum absolute value is observed in the interval of [0.6, 0.7] GeV/c

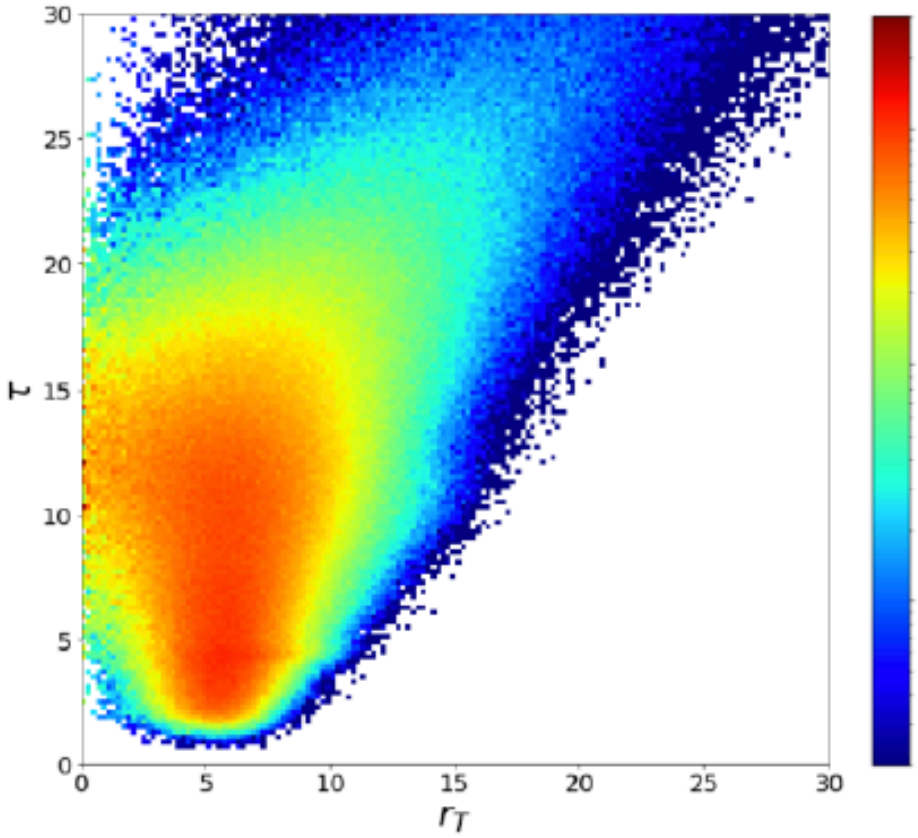

Maximum emission, τ_{max}, could be obtained from the fit:

$$g(\tau) \sim e^{-\frac{(\tau-\tau_{max})^2}{2\cdot d^2}}$$

where d - emission duration

To move to the distribution over τ, the r_T integration interval has to be selected

Interval over r_T is centered around the point of distribution maximum value

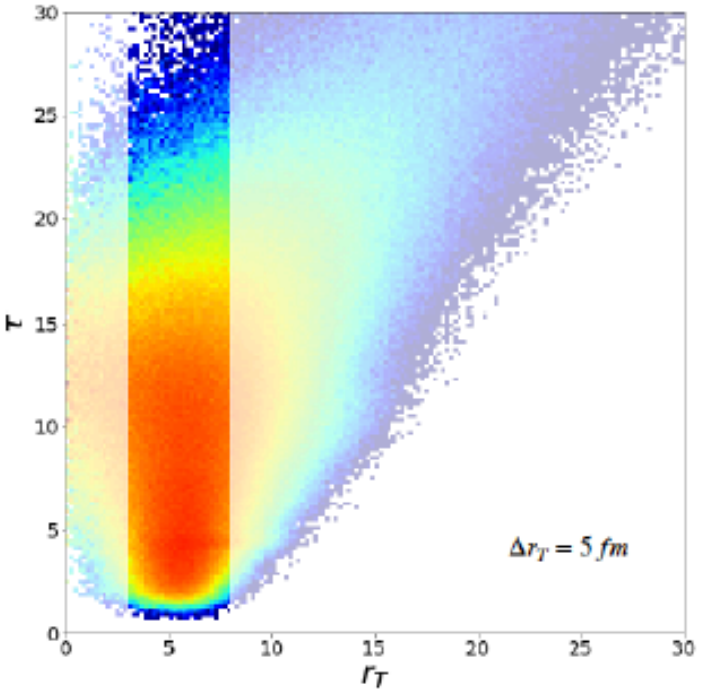

The 10% and 30% of points were truncated from the left and right distribution edge correspondingly, due to asymmetry of the distribution

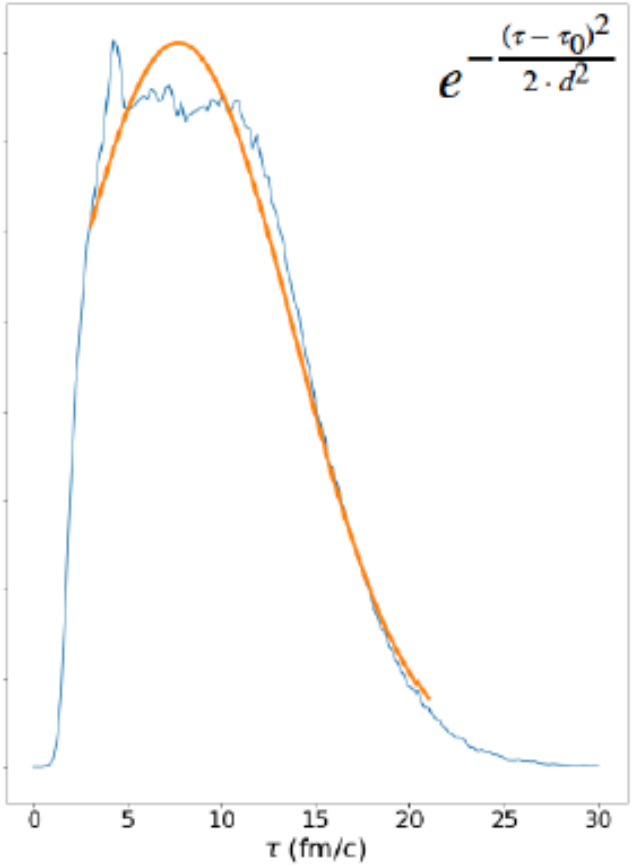

Different width of r_T regions were considered for extraction of τ.

r_T variation defines the uncertainty of the final value:

$$\tau = 7.03 \pm 0.88\ fm/c$$

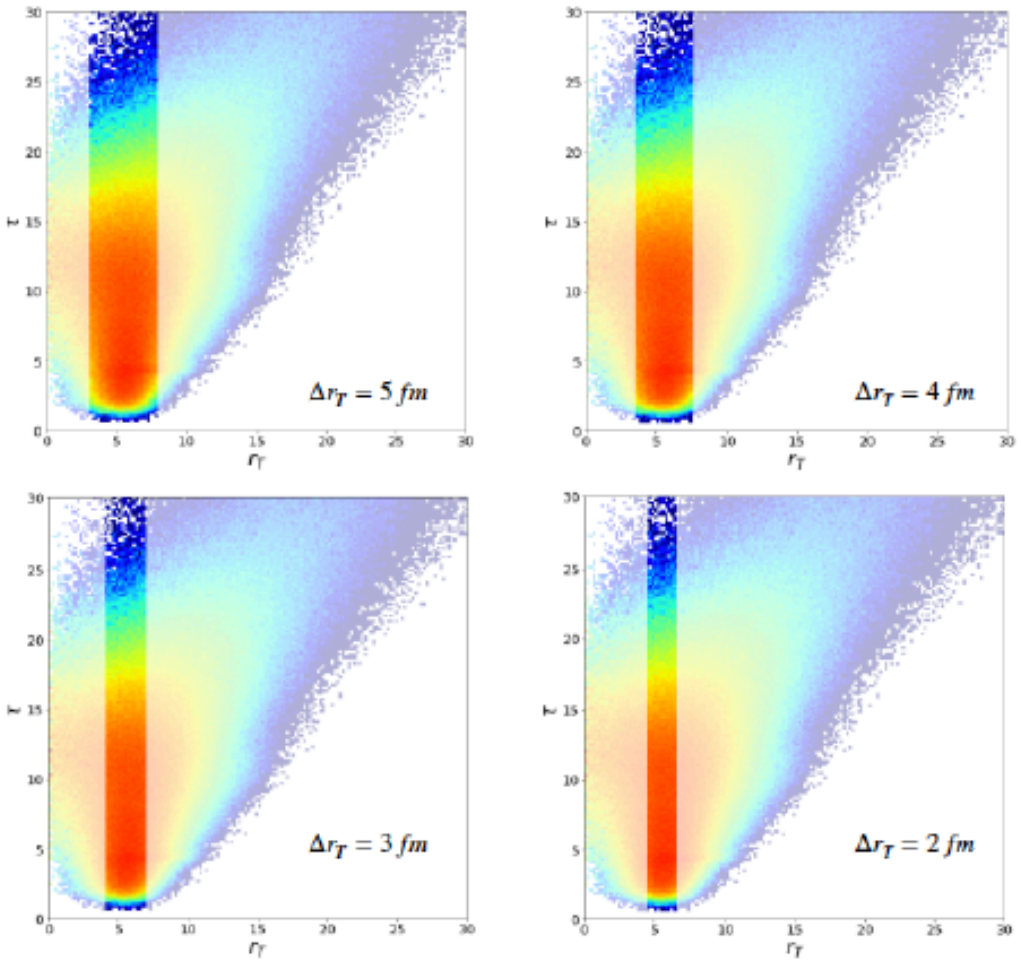

Comparison

Maximum emission time from correlation femtoscopy:

Fitting $R_{long} = \tau \cdot \sqrt{\frac{T}{m_T}}$

$$\tau = 7.13 \pm 0.04\ fm/c$$

Fitting R_{long} accordingly to Yu.Sinyukov et al., NPA 946 (2016) 227

$$\tau = 5.92 \pm 0.04\ fm/c$$

Maximum emission time from distribution of emission function:

$$\tau = 7.03 \pm 0.88\ fm/c$$

CONCLUSIONS

- *MC models favor chemical equilibration of hot and dense matter at $t \approx 7$ fm/c*
- *In MC models different hadron species are frozen at different times: K, π, anti-Σ, anti-p, anti-Λ, Λ and in different space regions with different values of T and chemical potentials*
- *These circumstances naturally explain such effects as*
  - *(i) normal directed flow for p, Σ, Λ and antiflow for their antiparticles at low and intermediate energy nuclear collisions*
  - *(ii) different polarization of Λ and anti-Λ in these collisions*
- *(iii) and many other peculiar signals and observables …*

Back-up Slides

Infinite hadron gas:
a box with periodic boundary conditions

BOX WITH PERIODIC BOUNDARY CONDITIONS

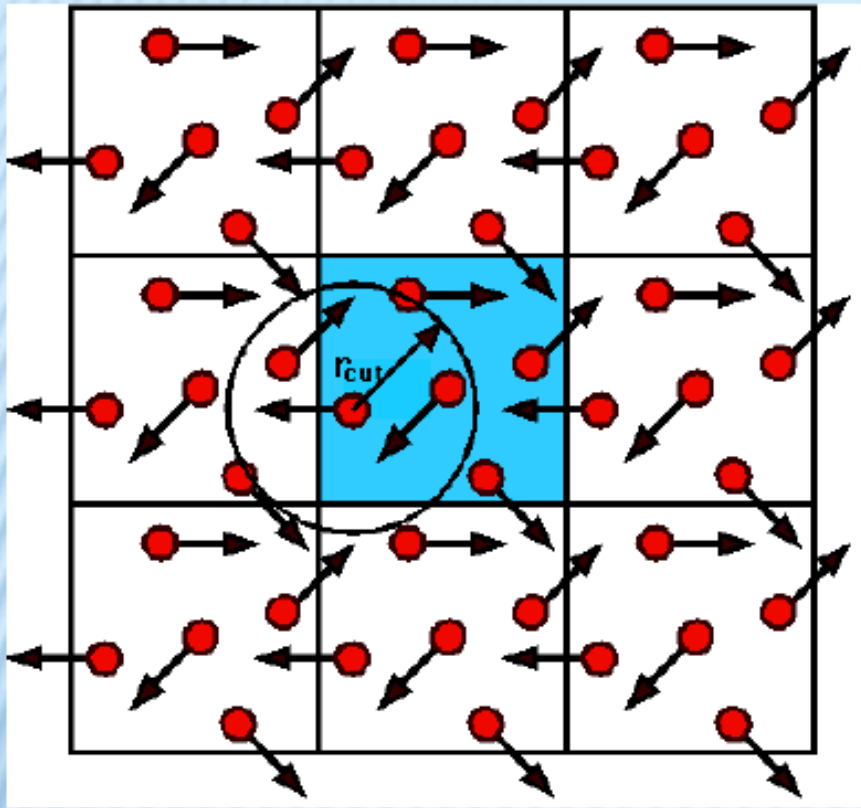

M.Belkacem et al., PRC 58, 1727 (1998)

Initialization: (i) nucleons are uniformly distributed in a configuration space;
(ii) Their momenta are uniformly distributed in a sphere with random radius and then rescaled to the desired energy density.

Model employed: UrQMD
55 different baryon species (N, Δ, hyperons and their resonances with $m \leq 2.25\ GeV/c^2$),
32 different meson species (including resonances with $m \leq 2\ GeV/c^2$) and their respective antistates.
For higher mass excitations a string mechanism is invoked.

Test for equilibrium: particle yields and energy spectra

BOX: PARTICLE ABUNDANCES

M.Belkacem et al., PRC 58, 1727 (1998)

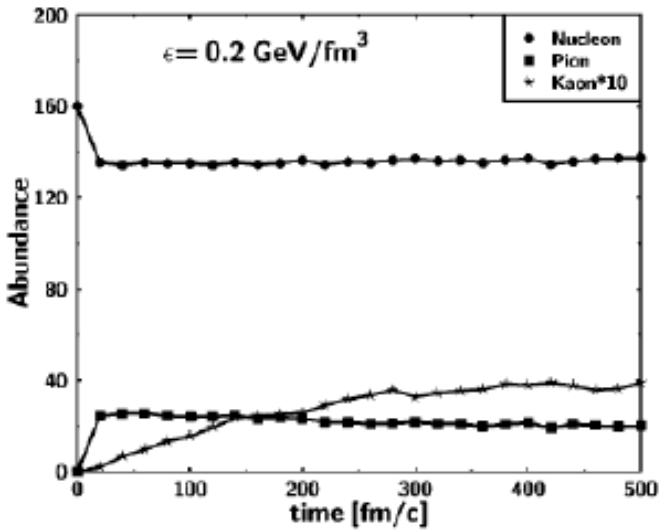

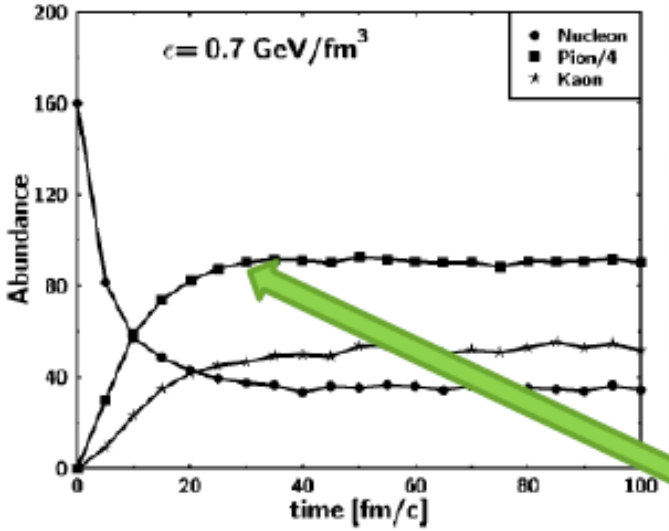

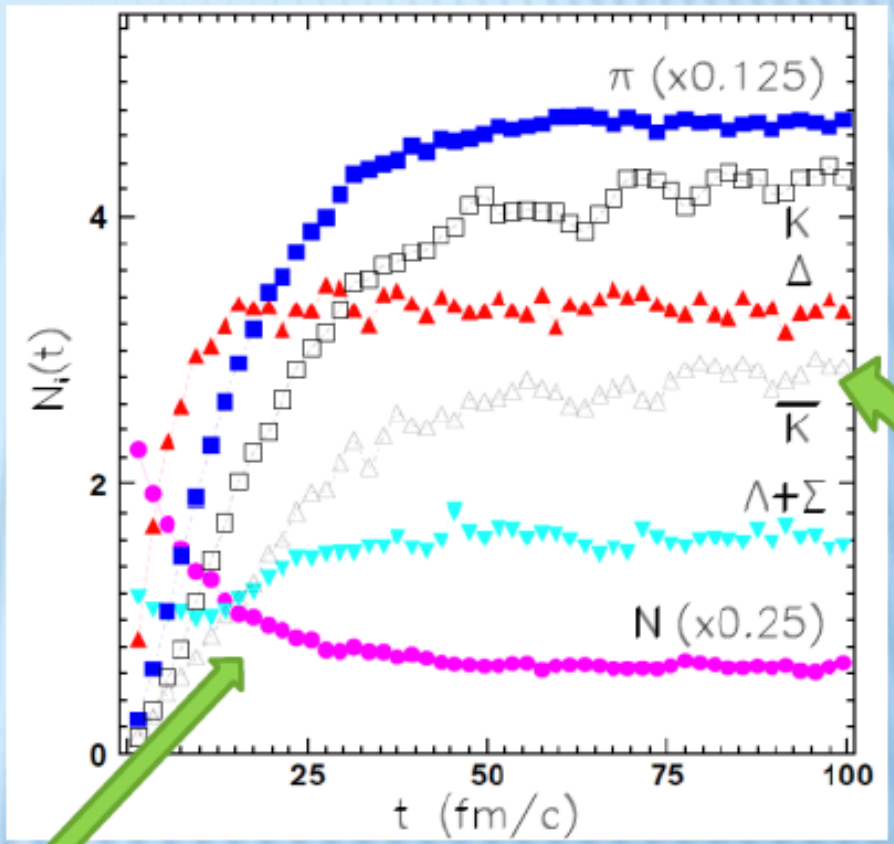

L.Bravina et al., PRC 62, 064906 (2000)

Saturation of yields after a certain time. Strange hadrons are saturated longer than others .

BOX: ENERGY SPECTRA AND MOMENTUM DISTRIBUTIONS

Fit to Boltzmann distributions ~exp(-E/T)

Fit to Gaussian distributions ~exp(-p^2/2mT)

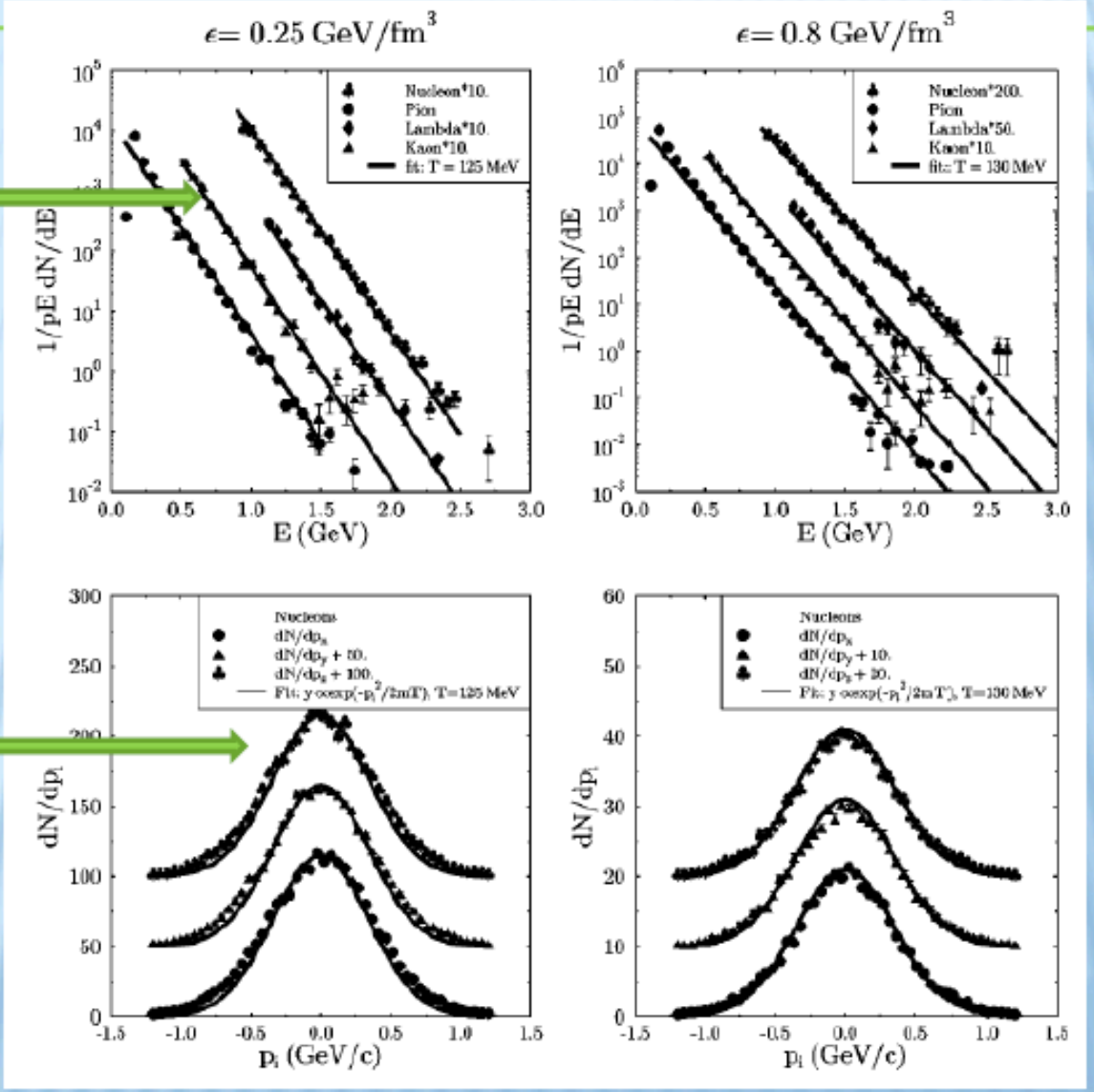

M.Belkacem et al., PRC 58, 1727 (1998)

Nearly the same temperature and complete isotropy of dN/dp_T

BOX: HAGEDORN-LIKE LIMITING TEMPERATURE

M.Belkacem et al., PRC 58, 1727 (1998)

HSD

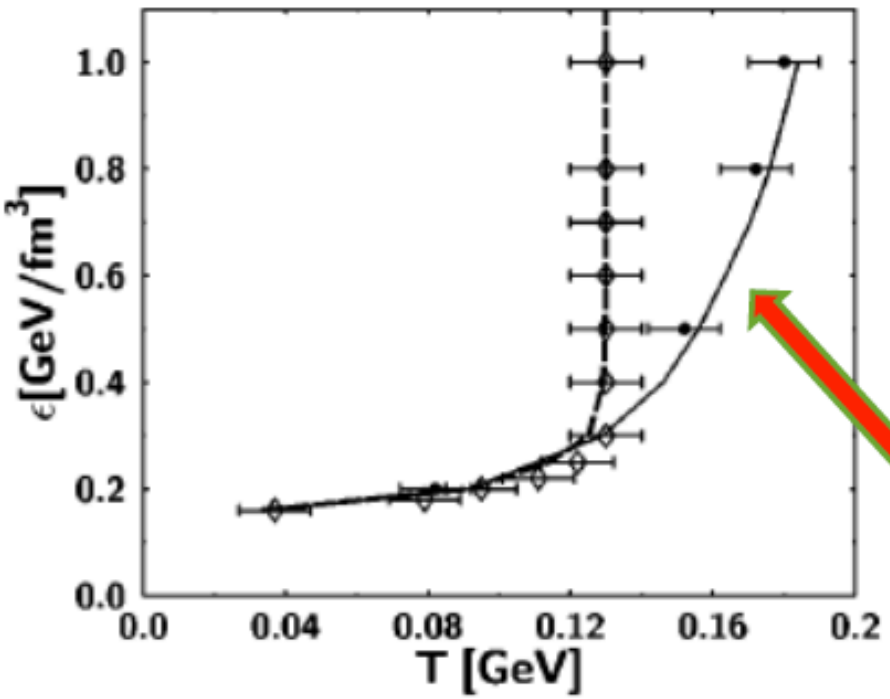

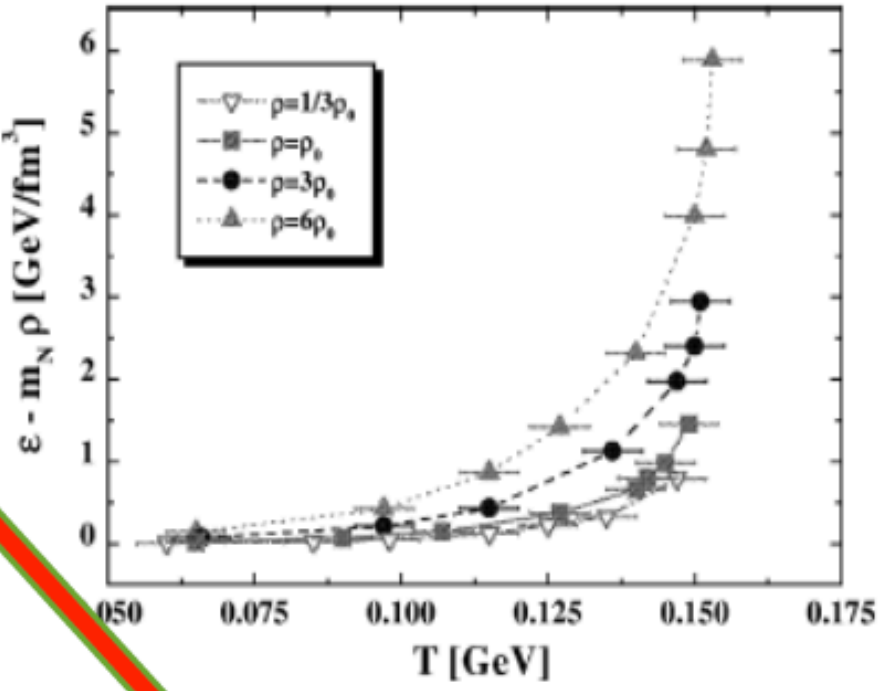

E.Bratkovskaya et al., NPA 675, 661 (2000)

UrQMD

A rapid rise of T at low ε and saturation at high energy densities. Saturation temperature depends on number of resonances in the model. W/o strings and many-N decays – no limiting T is observed.